Mapping of Sonochemical Reactors: Review, Analysis, and Experimental Verification

Parag R. Gogate, Prashant A. Tatake, Parag M. Kanthale, and Aniruddha B. Pandit
Chemical Engineering Division, Institute of Chemical Technology, University of Mumbai, Matunga, Mumbai 400 019, India

The erratic behavior of cavitational activity exhibited in a sonochemical reactor poses a serious problem in its design and scale-up. Several previous studies in the past dealt with mapping of sonochemical reactors, which have been critically analyzed and recommended for efficient scale-up strategies. There have been no efforts to link the primary effects (local pressure field) of ultrasound activity with the observed secondary effects (such as chemical reaction). In this work an ultrasonic horn (standard immersion-type reactor), and an ultrasonic bath (rectangular geometry with transducers located at the bottom in triangular pitch) reactors were mapped with the help of local pressure measurement (using a hydrophone), and liberated iodine was estimated using the Weissler reaction, and a quantitative relationship was established between the two. In estimating chemical reaction rates, the effect of microscopic variation in the type of microreactor used (test tube in this case) on the extent of degradation was also investigated. Measured local pressure pulses were used in theoretical simulations of bubble dynamics equations to check the type of cavitation taking place locally, and to estimate the possible collapse of the pressure pulse in terms of the maximum bubble size reached during the cavitation phenomena. A relationship also was established between observed iodine liberation rates and the maximum bubble size reached. The engineers can easily use these unique relationships in an efficient design, since the secondary effect can be directly quantified.

Introduction

Chemical effects associated with the cavitation induced in a liquid by the passage of ultrasound are quite distinct from the conventional chemical processes. Very high energy densities (energy released per unit volume) are obtained locally, resulting in high pressures (on the order of 100–50,000 bar) and temperatures (in the 1000–5000 K range), and these effects are observed at millions of locations in the reactor. There are larger illustrations where these spectacular effects have been successfully harnessed for a variety of applications worldwide. Few of the important applications can be given as chemical synthesis [in both homogenous and heterogeneous systems by way of increase in the rate and selectivity of many chemical reactions (Petrier et al., 1982, 1984; Pandit and Joshi, 1993; Mason, 1986, 1999; Petrier and Luche, 1987; Lindley and Mason, 1987; Shah et al., 1999; Thompson and Doraiswamy, 1999; Sivakumar and Pandit, 2001a; Sivakumar et al., 2002a)]: wastewater treatment [degradation of many of the biorefractory/complex chemicals (Cheung et al., 1991; Kotronarou et al., 1991, 1992; Petrier et al., 1992; Bhatnagar and Cheung, 1994; Serpone et al., 1994; Shirgaonkar and Pandit, 1997; Hua and Hoffmann, 1997; Seymore and Gupta, 1997; Weavers et al., 1998; Hung and Hoffmann, 1999; Pandit et al., 2001; Gogate, 2001)], textile processing (Thakore, 1990; McCall et al., 1998; Rathi et al., 1997; Yachmenev et al., 1998, 1999), biotechnology [cell disruption (Save et al., 1994; Shirgaonkar et al., 1998) and foam control in bioreactors (Ambulgekar et al., 2002)], and crystallization (Srinivasan et al., 1995). However, it should be noted that, in spite of extensive research, there is hardly any chemical processing being carried out on an industrial scale owing to the lack of expertise required in diverse fields such as material science, acoustics, and chemical engineering, for scaling up successful laboratory-scale processes, also due to the lack of a suitable reactor design and scale-up strategies.

Correspondence concerning this article should be addressed to A. B. Pandit.

Table 1. Overview of the Work in the Area of Mapping of Ultrasonic Reactors

Sr. No.	Reference	Details About Equipment and Measurement	Important Findings
1	Contamine et al. (1994)	• Cylindrical reactor with a circular single transducer located at the bottom of the reactor with a driving frequency of 20 kHz, acoustic power in the range 1–200 W, and another reactor with immersion transducer with the same ultrasonic generator as previous. Measurements in terms of physical effects (mass-transfer coefficients [MTC] using electrochemical probes) and chemical effects (rate of homogenous as well as heterogeneous reaction) of ultrasound over multiple locations in the reactor.	• Trends obtained for all the systems, that is, physical system, homogenous, and heterogeneous chemical reactions in terms of variation of cavitational intensity were similar. • For the ultrasonic reactor with transducer at the bottom, overall intensity decreases as we go away from the transducer with an intermediate increase at positions equivalent of multiples of $\lambda/2$. Also radial variation indicates maximum intensity at the center of the transducer with diminishing intensity away from the center. • For the reactor with immersed horn as a transducer, the profile was dependent on the power input. At higher power inputs, intensity diminishes with distance from the horn, whereas at low power input standing waves exist, giving an oscillatory profile. • The difference is attributed to very high power intensities (W/cm^2) in the case of immersion systems as compared to the system with the circular transducer at the bottom.
2	Soudagar and Samant (1995)	• Ultrasonic bath with driving frequency of 23 kHz, capacity 3 L, power input 120 W, three transducers at the bottom arranged in a triangular pitch, and a second bath with a configuration of 35-kHz frequency, capacity 2.75 L, and power input of 85 W with a single transducer at the center. Piezoelectric pressure intensity measurement probe (PPIMP) was used for measurement of local pressure intensity by recording genreated voltage on a cathode ray oscilloscope.	• The ultrasonic intensity diminishes with distance from the two transducers forming the base of the triangle, whereas intensity was slightly increasecd at distance $\lambda/2$ from the apex position transducer due to the overlapping of wave patterns. For the bath with a single transducer, the increased intensity is observed only above the center of the transducer. Thus, the triangular arrangement of transducers could be more useful as compared to a single transducer, as there is a large number of locations where a large intensity has been observed.
3	Chivate and Pandit (1995)	• Ultrasonic horn with driving frequency of 22.7 kHz and power input of 240 W through a horn area of 81 mm^2 with an energy transfer efficiency of only 2%. • Precalibrated aluminum foil of uniform surface mounted flat, parallel to the irradiating surface was dipped in test solution at various distances. The indentations produced were analyzed geometrically and the impulse pressure can be calculated.	• Pressures of several thousand atmospheres are observed very near the horn and decrease exponentially with the distance from the horn. Correlation is given for the estimation of pressure as Pressure (in atm) $= 9.82 \times 10^{-4}$ (distance in m)$^{-1.5}$ • Typical volume experiencing high pressures ($>10{,}000$ atm) was reported to be around 3 mm^3, which is a microfraction of the total volume, thus, limiting the large-scale applications of immersion systems. • Also the maximum pressure pulse observed is dependent on the vapor pressure of the medium used.
4	Romdhane et al. (1995a)	• Ultrasonic cleaner (parallelepiped tank with maximum acoustic power of 160 W, frequency of 26 kHz), hexagonal tank with each side fitted with a transducer, frequency of 22 kHz and consumed electric power of 300 or 600 W, sonitube with an aim of maintaining radial homogeneity (frequency of 20 kHz), and ultrasonic horn of operating frequencies 20 kHz and 40 kHz. • Cavitational intensity measurement using a thermoelectric probe by measuring the temperature difference between probe material temperature and the medium temperature.	• Standing waves have been observed in the ultrasonic cleaner, which increases the local cavitational activity. The ultrasonic power decreases as one moves away from the emitters. Increased activity has been observed at a distance equivalent to $\lambda/2$. Cavitational activity was found to be much more uniform in the case of hexagonal tank as compared to ultrasonic cleaner and uniformity was more at higher power inputs. • In the case of a sonitube, as the length of immersed portion increases, the ultrasonic activity has been found to increase due to the increase in the amount of energy being transmitted to liquid. The distribution of the intensity is fairly homogeneous in the radial direction. • For an ultrasonic horn, for both the frequencies, decreasing intensity with distance from the horn tip has been observed with increased activity at distances of $\lambda/2$. In the vicinity of the horn, bubbles have been observed that are responsible for the absorption of energy. The intensity also decreases in the radial direction away from the axis passing through center of the horn. • Comparison of different reactors using an efficiency factor reveal the highest homogeneity of cavitational activity for the sonitube (hence increased cavitation intensity) followed by the hexagonal tank.

Table continued

The major problems identified in designing large-scale reactors are the local existence of cavitation events very near the irradiating surface, wide variation in the energy dissipation rates in the bulk volume of the reactor coupled with the inability of the existing tools to accurately predict the cavitating zones in the reactor and link it with the observed chemi-

Table 1. (Continued) Overview of the Work in the Area of Mapping of Ultrasonic Reactors

Sr. No.	Reference	Details About Equipment and Measurement	Important Findings
5	Keil and Dahnke, 1996, 1997a,b; Dahnke and Keil, 1998a,b, 1999; Dahnke et al., 1999a,b	• Numerical simulations of the local pressure fields using different modeling approaches such as Helmholtz and Kirchhoff integral equation with homogeneous and inhomogeneous distribution of cavitation bubbles, consideration of the effects of small-amplitude sinusoidal oscillations of the gas bubbles present in the liquid. Different sonochemical reactors: one with simple cylindrical geometry with a circular ultrasonic transducer at the bottom (1), second a circular tube with open ends with irradiation with three ultrasonic horns placed in an equilateral triangle in the same plane around the tube (2), and the third one where an immersion transducer is used in a cylindrical vessel (3). Two different irradiating frequencies, 25 and 50 kHz, and the assumption of pure liquid have been considered in simulations.	• Cavitational activity was found to be maximum at the center axis of the transducer and diminishing away from the center line in the same plane, and also as one moves away from the transducers in a direction perpendicular to the tank bottom. For the case of homogeneous distribution of the bubbles, the influence on the pressure fields was negligible for a bubble fraction $<10^{-3}$, whereas above this a remarkable reduction in the pressure amplitude was observed. For reactors of types 1 and 3, intensity at the opposite end nearly vanishes, whereas considerable attenuation was observed for the reactor 2. For very high-volume fractions of gas/vapor (0.2), intensity vanishes even near the transducer surface. • For inhomogeneous distribution of the bubbles, which assumes very high bubble concentration near the ultrasonic source and lower concentration away from the source, the damping effect decreases considerably as compared to homogeneous distribution. For a volume fraction of 0.2, the acoustic field keeps its original structure in the vicinity of the beam source, decreases to a low value, and then an undamped propagation of intensity is observed due to low concentration away from source. Thus, decrease in intensity is only observed very close to the surface of the transducer. • An important characteristic of the findings that can be highlighted is that the active cavitation region is not a simple fraction of the transducer frequency or the amplitude. Thus, optimization needs to be done in terms of the number and properties of sound sources and properties of the liquid medium. • The trends in the pressure fields existing in the reactor obtained are quite similar to the earlier experimental results of Soudagar and Samant (1995), though quantitative agreement is not seen. The presence of the PPIMP transducer alters the sound field in its surroundings, and also additional standing waves are formed between the probe surface and the bottom of the reactor. This influence has not been considered in the theoretical simulations, which are also based on a number of approximations leading to inaccuracies.
6	Romdhane et al. (1997)	• Ultrasonic horn with driving frequency of 20 and 40 kHz and variable power input, ultrasonic cleaning tank with frequency of 26 kHz, maximum power input of 160 W, and two emitters at the bottom, sonitube operating at 20 kHz ensuring radial homogeneity of the ultrasound. Experimental measurement of local ultrasonic intensity using thermoelectric probes in a reactor of capacity 5 L.	• For horn-type reactors, the ultrasonic activity decreases as we move away from the central axis of the horn with a small increase in the activity at distances corresponding to $\lambda/2$. For ultrasonic cleaner a cavitational threshold was observed at 25-W power input. Power consumption has little effect on the trend in the variation of local ultrasonic activity. • The ultrasonic intensity was found to be dependent on agitation as well as circulating fluid Reynolds number (lower activity at higher values, which indicates the disturbance of the sound field existing in the reactor; the contribution of standing waves will also be lower at higher values of the Reynolds number). Also the presence of solid particles or cavitation bubbles attenuates the ultrasonic wave propagation. Optimization in terms of the size of the solid particles and the volume fraction needs to be done to get a proper balance between the change in the ultrasonic activity and the reaction or extraction requirements. For example, the presence of solid particles decreases the local ultrasonic activity but at the same time enhances the cavitational activity in terms of a number of cavitational events possibly due to surface cavitation.

Table continued

Table 1. (Continued) Overview of the Work in the Area of Mapping of Ultrasonic Reactors

Sr. No.	Reference	Details About Equipment and Measurement	Important Findings
7	Gonze et al. (1998)	• Different reactor configurations varying in terms of the arrangement of transducers and reflectors for formation of standing waves with capacity in the range of 1 to 6 L, acoustic power input in the range of 1 to 100 W. Local effects were measured with the help of jacketed thermocouples.	• Maximum temperature sensed by the thermocouple in the case of a juxtaposed emission module (JEM) and directed-beam module (DBM) was observed above the center position of the transducers, whereas the temperature gradually decreased as one moves away from the center axis. Thus, the active volume is restricted to just the cylinder above the transducer. With combined emission modules (CEM), where the two ends of the cylinder are fitted either with one transducer and one reflector or transducers at each end, complete overlapping of the reaction zones is observed. Similar trends were observed with the measurements of chemical effects by chemiluminescence of luminol. • Geometry was optimized in terms of the length between two transducers or transducer and reflector to obtain the beneficial effects of standing waves. The rate constant for the degradataion of NaPCP observed in DBM, where standing waves are formed, is about 25% more as compared to the JEM.
8	Faid et al. (1998)	• The ultrasonic device used is a sonitube with a driving frequency of 20 kHz, and a 20-kW Branson-made generator. Solution is pumped through the reactor, and the active length is 37.5 cm. • Cavitational activity was measured with different probes viz. the thermoelectrical probe (relative temperature difference measurement), electrochemical probe (measurement of mass transfer coefficient), the chemical probe (measurement of rate of decomposition of KI).	• The method used for measurement of cavitational activity does not affect the observed trends. The ultrasound effects vary significantly along the axis of the resonant tube (increases from the bottom of the tube due to the formation of standing waves in the resonant tubular emitter), but an almost negligible variation is observed along the radial direction, that is, from the tube axis to the wall. Thus, the sonitube reactor gives a radial homogeneity. • In the sonitube-type reactor, where the liquid is pumped through an irradiation zone; some ultrasonic activity is also observed in the region beyond the irradiation zone. In the irradiation zone, the activity has been observed to be minimum at the lower extremity and increases as we move away from the lower end. • The electrochemical method is found to be more sensitive toward the variation in ultrasonic activity (4 times the variation in the minimum and maximum values) as compared to the other two methods (only 2 times the variation).
9	Dahlem et al., (1998, 1999)	• Telsonic horn (radially vibrating horn with supplied power of 1000 W, 20 kHz driving frequency, and irradiation area of 365 cm^2) and laboratory-scale horn (with longitudinal vibrations, power-300 W, driving frequency of 20 kHz, and emitting surface of 0.8 cm^2). • Hydrophone probe used for mapping of local acoustic field; local measurements with the extent of iodine liberation from the Weissler reaction.	• Maximum activity at a distance equal to half the wavelength for the pressure amplitude measurement (only subharmonic pressure amplitude has been considered, which does not show the realistic picture). The maxima for pressure measurements coincide with those obtained for the iodine liberation, indicating correspondence between the two. Large intensity was observed below the horn with Weissler reaction rates about 50% higher as compared to the maximum obtained along the radial locations, and also PIV measurements give velocity of fluid due to acoustic streaming 6 times higher at the position below the horn. Similar measurements with a laboratory horn indicate the active region is in close proximity to the horn. Sonochemical yields are higher for the telsonic horn as compared to the conventional laboratory-scale horn.
10	Moholkar et al. (2000)	• Ultrasonic cleaning bath with a driving frequency of 22 kHz, power input of 120 W, and liquid capacity of 300 mL. Pressure measurements using a hydrophone at different locations in the reactor. • Experimental runs were performed with two liquids, one cavitating (water) and other noncavitating (silicon oil) to clearly estimate the quantity of the pressure pulse due to cavitation.	• The cavitation intensity is concentrated at the center of the bath while it decreases considerably at the corners and the edges of the bath. This can be attributed to the conical divergence of the acoustic waves in the bath generated by the transducer located at the bottom in the triangular pitch. Also the intensity diminshes as one moves away from the source. • The measured pressure amplitude was used in the theoretical simulations of the bubble dynamics using the Gilmore model, and it was shown that bubbles at locations of a minimum cavitation intensity show stable cavitation, whereas bubbles at maximum cavitation intensity show transient cavitation, which indicates that such locations will be beneficial for the chemical reactions.

Table 1. (Continued) Overview of the Work in the Area of Mapping of Ultrasonic Reactors

Sr. No.	Reference	Details About Equipment and Measurement	Important Findings
11	Moholkar and Warmoeskerken (2000)	• Numerical simulations for the bubble dynamics studies using the Gilmore model based on the Kirkwood–Bethe hypothesis. A hypothetical dual-frequency reactor has been considered for the analysis.	• Transient collapse of the bubbles has been observed only if the phase difference between the two waves is either $\lambda/2$ or $-\lambda/2$ and the second or the coupling frequency is either the first subharmonic or ultraharmonic of the first or main frequency. Moreover, mapping of the reactor shows that there is no transient cavitation close to the transducer surface, which means that there will be minimal erosion of the surface under application of dual frequencies. Optimization can be done in terms of the operating parameters of the two waves, namely, phase difference, individual frequencies, and/or acoustic power input.

cal or physical effects of cavitation, and, last, erosion of the sonicator surfaces at the high power intensities required for industrial-scale operations. In some previous works (Gogate, 2001; Gogate et al., 2001a,b), we have tried to address the first problem by using a new geometric arrangement of the transducers on the irradiating surface. The experimentally obtained energy efficiencies and the cavitational yields have been found to be more the conventional immersion systems, that is, ultrasonic horn with the scale of operation as high as 1.5 L in a dual-frequency flow cell (Sivakumar et al., 2002b; Gogate et al., 2001a), and 7.5 L in a hexagonal triple-frequency flow cell (Gogate et al., 2001b).

The second problem is mainly attributed to the current state of the transducer technology and the attenuation of the acoustic field by cavitation events at and near the sonicator surface. Cavitation is induced in a sonochemical reactor by the passage of ultrasound. This ultrasound is produced by transducers, which convert the electrical energy into mechanical energy (vibrational energy). These transducers are strategically located on the reactor sidewall or at the bottom of the tank. Due to this, the cavitational activity is concentrated in the zones closer to the transducer surface, resulting in spatial variation of the cavitational activity. Also due to the attenuation of ultrasound, there is a decrease in the cavitational activity away from the transducers. It is of paramount importance to understand the effect of these changes on the cavitational activity, which results in active and passive zones in the reactor. Hence, it becomes necessary to characterize the cavitational activity and to study its spatial variation. From the current level of knowledge in the area of sonochemical reactors it is impossible to accurately predict the active and passive zones in the reactor, though the group of Keil and coworkers has done some very good work in this area, as discussed in detail later. In the present work, we also have tried to identify the active and passive zones with the help of a mapping exercise and link these driving pressure fields with the observed chemical effects in terms of the yields of iodine from the Weissler reaction.

The third major problem identified in the efficient scale-up of the ultrasound-based reactors is more dependent on the availability of knowledge from the field of material science. The aim should be to develop new transducers with a material of construction giving minimal erosion rates at higher power dissipation levels and at the same time with similar levels of energy transfer for cavitation events. Moreover, transducers with concave surfaces for irradiation can also be developed, which results in focusing of energy at locations other than the transducer surface, leading to minimal erosion rates at the irradiating surface. Such designs can be effectively used at higher scales of operation where because of high levels of power dissipation, the erosion rates may be very high in conventional flat designs. Magnetostrictive transducers need a special mention here: these can be operated at much higher levels of power dissipation, which is a necessity when a large-scale operation is considered. They can be easily used in gases as well as liquids. Moreover these systems can be cooled by a jet of cold water focused on the vibrating system or be completely water-cooled, and hence greater outputs can be obtained, plus continuous operation of the ultrasonic equipment is also possible for longer time periods. A further advantage is that these models can be sterilized for chemical or medical work.

In this work, we have made an attempt to give an overview of the literature available in the area of mapping cavitational activity, and based on the analysis of the same, we give some recommendations about efficient scale-up in terms of the location of the transducers, location of the reaction medium relative to the transducers, and so on, and we propose some guidelines for future work. Furthermore, the variation in the cavitation intensity has been studied in two different sonochemical reactors that differ in terms of the placement of the transducers, viz., ultrasonic bath (three transducers placed at the bottom of the reactor) and an ultrasonic horn (single immersed transducer). The present work aims at local measurements of the pressure amplitudes using a hydrophone, measurement of the chemical effect of cavitation, that is, the extent of decomposition of the aqueous KI solution at the same locations and relating the observed cavitational yields with the measured pressure fields, and also with the theoretical predictions of the bubble dynamics under the experimental conditions at different locations using the Tomita Shima equation (Shima and Tomita, 1979, and Tomita and Shima, 1986), which considers the compressibility of the medium at the later stages of collapse, and hence is more realistic in comparison to the Rayleigh–Plesset equation, which ignores the liquid compressibility effects.

Critical Analysis of the Existing Literature

In the past, attempts have been made to understand the uneven distribution of the cavitational activity existing in the reactor. Table 1 summarizes these findings in terms of the technique used, type of the reactor considered, and important results obtained in the studies. It can be seen that these studies tried to identify the primary (measurements in terms of pressure amplitudes or the local temperatures), or the sec-

ondary effects (either physical [measurement of mass-transfer coefficients] or chemical [sonoluminescence and Weissler reactions]) of the wave propagation in the medium either based on experimental work or rigorous theoretical simulations. The following important considerations for developing an effective scale-up strategy can be highlighted based on the detailed analysis of the findings as illustrated in Table 1.

1. A wide distribution of the cavitational activity exists in the sonoreactor, with the maximum intensity observed just above the center of the transducer (for the standard arrangements such as ultrasonic horn/bath). The intensity varies both axially and in the radial direction with decreasing trends as we get further away from the transducer (in the axial direction) and away from the axis passing through the center of the transducer (in the radial direction). The intensity has been found to increase by a small amount at distances corresponding to $\lambda/2$ in the axial direction, where λ is the wavelength of the driving sound source (Pugin, 1987; Romdhane et al., 1995a; Romdhane et al., 1997; Dahlem et al., 1998, 1999). Similar results also have been obtained in the present work.

2. Immersion types of transducers are the poorest, when scale-up possibilities are considered, though very high intensities (pressures of the order of few thousand atmospheres) are observed very near to the horn. The intensity decreases exponentially as one moves away from the horn and vanishes at a distance of as low as 1 cm, as observed by Chivate and Pandit (1995). It also should be noted that the active zone in the case of the ultrasonic horn also depends on the maximum power input to the equipment as well as the operating frequency. Romdhane et al. (1995a) have shown that the ultrasonic activity falls from a maximum 120°C temperature difference measured with a thermal sensor to less than 10°C within a distance of 1 cm for the ultrasonic horn with an operating frequency 20 kHz and $P_{max} = 160$ W, whereas for another horn with an operating frequency 40 kHz and $P_{max} = 600$ W, the distance required is around 2 cm for the same overall drop. Thus, using higher power dissipation does not directly result in increasing the active cavitation volume (approximately a four times increase in power dissipation results in only a two times increase in the active volume). Furthermore, the ultrasonic activity in the radial plane passing through the tip of the horn diminishes at a distance of 3 cm away from the axis through the center of the vibrating area. Thus, the active zone is restricted to a small zone around the irradiating surface. Using the PIV technique and with the help of numerical models (Dahlem et al. (1998, 1999) have found the local velocities due to acoustic streaming existing near the surface of the ultrasonic horn. They have reported that the active zone is restricted to near the surface only, and very low velocities are obtained at the bottom of the reactor as well as near the reactor wall in the radial direction.

3. In the case of the ultrasonic bath, when the bottom of the reactor is irradiated with a single transducer, the active zone is restricted to a vertical plane just above the transducer with the maximum intensity at the center of the transducer. Thus, the area of irradiating surface should be increased so as to get better distribution/dissipation of energy in the reactor. This has the dual advantage of decreased ultrasonic intensity (defined as power dissipation per unit area of the irradiating surface), which increases the magnitude of the pressure pulse generated at the end of the cavitation events (Gogate and Pandit, 2000). In an earlier work (Gogate et al., 2000a), it was also shown, using decomposition of KI as the model reaction, that for similar operating frequencies, the ultrasonic bath gives better cavitational yields [defined as iodine liberation per unit power density (watts/m^3) of the equipment] as compared to the ultrasonic horn. Mujumdar et al. (1997) have also obtained similar results with emulsification reactions. Dahlem et al. (1998, 1999) have shown better local ultrasonic intensities and iodine liberation rates for the radially vibrating horn (1,000 W dissipated through a 365-cm^2 area) as compared to a conventional horn (longitudinal vibrations, 300 W dissipated through a 0.8-cm^2 area).

4. To increase the active zones existing in the reactor, one can easily modify the position of the transducers (if multiple transducers have been used, which is likely to be the case for a large-scale operation, because it is quite difficult to successfully operate a single transducer with very high power and frequency due to the limitations of the construction materials for the transducers), so that the wave patterns generated by the individual transducers will overlap, which also results in uniform and increased cavitational activity. Arrangements can be constructed, such as triangular pitch in the case of the ultrasonic bath (Soudagar and Samant, 1995; Dahnke and Keil, 1998a,b), tubular reactors with two ends either irradiated with a transducers or one end with a transducer and the other with a reflector (Gonze et al., 1998), parallel-plate reactors with each plate irradiated with either the same or different frequencies (Thoma et al., 1997; Gogate et al., 2001a,b), and transducers on each face of a hexagon (Romdhane et al., 1995a; Gogate, 2001; Gogate et al., 2001b). It is of the utmost importance to have uniform distribution of the ultrasonic activity in order to get increased cavitational effects. Romdhane et al. (1995a) have compared different ultrasonic equipment and have shown that a hexagonal reactor with a single transducer at each of the hexagon's faces gives better homogeneity as compared to conventional ultrasonic horn and parallelepiped geometry. The uniformity of the distribution can be further increased by using multiple transducers on the face of the hexagon (Gogate et al., 2001b). Thus, newer designs giving uniform and enhanced ultrasonic activity over the entire region of the cavitational reactor, must be developed.

5. The work of Keil and coworkers (Keil and Dahnke, 1996; Keil and Dahnke, 1997a,b; Dahnke and Keil, 1998a,b, 1999; Dahnke et al., 1999a,b) appears to be pioneering in terms of simulations of the pressure fields existing in the reactor. Such a detailed analysis can be used to identify the regions with maximum pressure fields in a large-scale reactor, and then perhaps small reactors can be placed strategically at these locations in order to get maximum benefits. It might happen that the threshold required for certain applications is obtained at these locations, but if considered globally, these effects will be marginalized, resulting in much lower yields from the cavitation reactors. Thus, the location of the transducers on the irradiating surface and the location of the microreactors will also depend on the type of application, which determines the required cavitational intensity. It should be noted that a one-to-one correspondence between the simulated pressure fields and the experimental reactions must be established before reaching any firm conclusions. In the later sections, the simulated conditions using the bubble dynamics equations have been correlated with the observed cavita-

tional yields for the decomposition of KI, which illustrates the methodology to be followed in establishing the correspondence for the specific applications.

It also should be noted that there is some room for improvement in the models used by Keil and coworkers. The homogenous density distribution of the bubbles as assumed in the work (Dahnke and Keil, 1998a) is difficult to achieve, even in a well-stirred ultrasound bath. In addition, bulk movement of the liquid in the bath due to stirring or acoustic streaming can disturb the pressure fields due to the scattering of ultrasound waves. In the simulation with inhomogeneous distribution of the bubbles (Dahnke and Keil, 1998b, 1999), the assumption of homogenous bubble distribution in one plane (radial variation of bubble size and number has been neglected) also is not possible practically, since the bubble volume fraction changes continuously with sound-wave propagation due to continuous generation and collapse of the cavities, plus the number of these cavities varies with time. Also, the assumption of small-amplitude sinusoidal motion in the modified wave equation is questionable, especially in the case of pressure waves with much higher amplitudes (>1 atm), which are again likely to be used at higher scales of operation.

Nevertheless, this work surely cannot be underestimated and can be taken as a starting point for obtaining a clearer picture of the cavitation phenomena. Also, experimental verification of the obtained simulated pressure fields and their effects on the physical and chemical effects of ultrasound needs to be established. Simple techniques that can be used for the said measurements can be thermochemical/electrochemical probes (Contamine et al., 1994; Trabelsi et al., 1996), thermoelectrical probes (Romdhane et al., 1995b; Romdhane et al., 1997; and Faid et al., 1998), thermister probes (Martin and Law, 1980), thermocouples (Gonze et al., 1998), sensors based on piezoelectric effect (Soudagar and Samant, 1995; Dahlem et al., 1998, 1999; Moholkar et al., 2000; the present work), colorimetric measurements (Ratoarinoro et al., 1995), chemical reactions, such as the fading of color intensity of phenolphthalein (Rong et al., 2001), sonoluminescence of luminol (Gonze et al., 1998), decomposition of KI (Weissler, 1950; Contamine et al., 1994; Faid et al., 1998; Dahlem et al., 1998, 1999; the present work), PIV measurements for the local velocity due to acoustic streaming (Dahlem et al., 1998, 1999), Michael reaction (Contamine et al., 1994), and so on. Faid et al. (1998) have compared different sensors that can be used for the measurements of local cavitational effects, namely electrochemical, thermoelectrical, and chemical probes, and have shown that the results of cavitational distribution are the same irrespective of the type of sensor used for the measurement.

6. The use of multiple frequencies results in a relatively better distribution of cavitational activity and provides a better scale-up option. As pointed out by Dahnke and Keil (1998a), to obtain a better energy distribution one has to modify the sound source in terms of the number and properties, and in this context multiple frequencies even offer enhanced flexibility. Moholkar et al. (1999) and Moholkar and Warmoeskerken (2000) have also shown that by adjusting the phase difference and magnitude of two waves, transient cavitation can be obtained at increased reactor sites, which results in better overall cavitational activity. Moreover, due to the use of multiple frequencies, the violent collapse of the cavities is restricted near the transducer surface, resulting in a decreased erosion of the surface (Moholkar and Warmoeskerken, 2000), which was another major problem in the scale-up as outlined earlier. In the earlier works, it was also shown using different chemical reactions [decomposition of KI (Gogate et al., 2001a), destruction of *p*-nitrophenol (Sivakumar et al., 2002b), destruction of rhodamine B, a typical effluent in the effluent from the dye industry (Sivakumar and Pandit, 2001b), degradation of formic acid (Gogate et al., 2001b)], that the reactors based on multiple frequencies give better results compared to single-frequency reactors. Moreover, Tatake and Pandit (2002) have also indicated, with the help of numerical simulations of bubble dynamics using the Rayleigh–Plesset equation, that the collapse of cavities is more violent for the case of multiple-frequency systems than for a single operating frequency of the same or twice the intensity.

7. Dahnke and Keil (1998a) have also shown that merely increasing the acoustic power input to the reactor or increasing the transducer frequency cannot enhance/improve the distribution of the cavitational activity. Romdhane et al. (1997) have also reported that the local ultrasonic intensity, as measured with the help of thermoelectric probes, remains unchanged with increasing power input (in the range 12.5 W to 39 W). Thus, increasing the power input to the reactor in order to achieve higher cavitational yields certainly cannot be a good scale-up strategy. The experimental evidence (Couppis and Klinzing; 1974; Gutierrez and Henglein, 1990; Ratoarinoro et al., 1995; Ondruschka et al., 2000), indicating that an optimum power input is always required for a particular reaction beyond which the beneficial effects are not observed also confirm this. A detailed discussion about the optimum intensity has been already presented in an earlier work (Gogate et al., 2001a).

8. The local ultrasonic activity is also dependent on the agitation, the presence of solids (size and volume fraction), or the flow regimes used in the circulating type of reactor (liquid, which passes through a zone of ultrasonic irradiation and back to the storage tank is being pumped at a definite rate). In a recent work carried out in this department, a dual-frequency flow cell was operated in a continuous loop and in combination with the hydrodynamic cavitation reactor (orifice plate setup; for details refer to Gogate et al., 2001a), in order to increase the active cavitational volume in the reactor and examine the synergism between the two different types of cavitation. The cavitational yield due to the combined operation of the dual-frequency flow cell and hydrodynamic cavitation setup depends not only on the individual contributions but also on the synergism between the two. Preliminary results indicate that the rates of iodine liberation at higher recirculation flow rates were lower in comparison to the operation with lower flow rates, indicating that the contribution of the ultrasonic irradiation to the overall cavitational effect at higher flow rates is possibly due to the lower disturbance of the sound field existing in the reactor. This fact is further confirmed with the observation of higher cavitational yields at increased flow rates for the case of a hydrodynamic cavitation setup alone (Vichare et al., 2000). Also, Romdhane et al. (1997) have shown that the local ultrasonic activity decreases with agitation as well as with an increase in the Reynolds

number (defined as $= d \times v \times \rho/\mu$, where ρ is the liquid density, μ is the viscosity, v is the recirculation velocity, and d is the inner diameter of the equipment used). Moreover, the peaks observed at distances of $\lambda/2$ in the case of a stagnant liquid medium diminish in the case of an agitated medium, thereby confirming the disturbance caused in the propagation of the sound wave. Similar results were obtained in another setup where the liquid was recirculated through the irradiation zone. To give a quantitative idea, an increase in the Reynolds number from 219 to 10,656 decreases the measured temperature difference from 121.5°C to 7.6°C, indicating that there is an almost linear effect of the Reynolds number on the ultrasonic activity. A quick analysis of the data given in the work indicates a temperature difference of around 127°C if the fluid was stagnant (Temperature difference $= -0.01 \times$ Reynolds number $+ 127$ with an R^2 value for the equation fitting of 0.95). It must be noted that the mathematical relationship only gives an indication of the effect of the recirculation flow rate on the cavitational activity and may not be linear in all the cases. The effect of the flow regime can also be linked to the standing-wave pattern existing in the reactor due to the reflection of sound waves, which also contributes to the enhancement of cavitational activity. At higher operational flow regimes, standing waves will necessarily be destroyed. However, the exact effect of the flow regime on the propagation of the sound wave and sound field existing in the reactor is not well understood; still, it can be said that for getting enhanced benefits from the continuous operation of sonochemical reactors, one should operate with as low flow rates as possible for single-phase operations.

Nevertheless, this is a very important point that needs to be considered, particularly for applications involving multiple phases such as chemical reactions and solid–liquid extraction. On one hand, where the increased agitation or Reynolds number results in less cavitational activity, it also results in better mixing of the two phases, which might enhance the rates. The same trend was observed with the size and the volume fraction of the solid particles present. The higher size particles were observed to attenuate the wave propagation to a lesser extent, whereas smaller size particles give better interfacial areas for chemical reactions as well as extraction. Also, an increase in the volume fraction results in lower local ultrasonic activity, but may have a positive effect on the cavitational activity (additional surface, and hence a larger number of nuclei for the cavitation phenomena), and also on the chemical reactions where the solid particles used are acting as a catalyst for the reaction. Thus, optimization needs to be made taking the two opposite effects into consideration.

9. For better scale-up possibilities with the ultrasonic reactor, it is also important to design new reactors, which can be operated in continuous mode. The traditional immersion or ultrasonic bath-type reactors cannot be operated in continuous mode with high cavitational yields. Romdhane et al. (1995a) and Faid et al. (1998) have described a sonitube reactor, which can be operated in a continuous manner. Mapping of this reactor shows some cavitational activity even beyond the irradiation zone. Moreover, as compared to various reactors studied in their work [ultrasonic horn, ultrasonic cleaner (bath), hexagonal reactor], sonitube gives a better homogeneity in terms of the cavitational activity; negligible variation has been reported in the radial direction. The two- and three-frequency flow cells designed in this department can also be operated in a continuous manner, which forms a part of the future investigation. In the case of continuously operated sonochemical reactors, the selection of operating flow rates is a crucial factor, particularly for the multiphase systems, as discussed in details earlier.

The design used by Dahlem et al. (1998, 1999) also needs a special mention here. The telsonic horn, which has radial vibrations instead of conventional longitudinal vibrations, for the immersion system has the double advantage of a higher irradiating surface (lower intensity of irradiation, resulting in better yields) coupled with good distribution of the energy in the radial direction. Moreover, even if the horn is radially vibrating, local measurements just below the horn also show high cavitational activity, which again will be more beneficial in enhancing the global sonochemical yields.

The preceding analysis of the existing literature also shows that all these studies have not conclusively established the basis for how the variation in the local cavitational activity affects the overall performance of the reactor, and there is no relationship between the primary (development of a local pressure/temperature pulse) and secondary (observed positive effects for the particular application, such as the chemical reaction rates, in the case of chemical synthesis) effects of the ultrasound action. We tackle this problem in the following sections.

Two of the most important parameters, which can be directly related to the secondary effects, are the driving pressure and the cavity collapse pressure generated in the acoustic field, which are also a function of the maximum radius reached by the cavity nuclei in the growth stage. In the present work, the local pressure intensity was measured using a piezoelectric hydrophone. The advantage of using a hydrophone over other pressure measurement techniques is that the hydrophone gives both the local and the real-time pressure intensity in addition to the information on the frequencies characterizing the pressure pulses. Calorimetric methods employing highly sensitive thermocouples or other techniques cannot provide this information. Also, hydrophones have better spatial resolution, bandwidth, and sensitivity compared to the other pressure measurement techniques. The dimensions of the hydrophone were such that it did not significantly affect the existing acoustic pressure field. Detailed discussions about the different measurement techniques used for mapping ultrasonic intensity can be readily obtained in the open literature (Neppiras, 1968; Saksena, 1983; Mason and Lorimer, 1988; Suslick, 1988).

It is also important to understand how the variation in this local pressure intensity affects the reaction rates; hence, the chemical reaction rates at different locations were measured using a model reaction as the decomposition of potassium iodide (KI) to give iodine. A detailed experimental procedure for these measurements is discussed in the following section.

Experimental Methodology

Experimental system

As was said earlier, two different experimental systems differing in the placement of the transducers were used in the present work. The first experimental system used was a stain-

less-steel low-powered ultrasonic bath (Dakshin Ltd., Mumbai, India; maximum power rating, 120 W, and driving frequency, 20 kHz) with internal dimensions of length = 0.15 m, breadth = 0.15 m, and height = 0.15 m. The bath has three transducers located at the bottom, arranged in a triangular pitch, as shown in Figure 1. The calorimetrically measured actual power input to the system (by measuring the temperature rise in uncontrolled operation; for details see Gogate et al., 2001a) was found to be equal to 36 W, indicating an energy transfer efficiency of 30%. The second is a typical immersion-type system (Dakshin Ltd., Mumbai, India; maximum power rating, 240 W, and driving frequency, 20 kHz) with a tip diameter of 2 cm and was always dipped in 2 cm below the liquid level. The energy efficiency of the Dakshin horn was found to be a mere 3%, which is quite a bit lower than the ultrasonic bath (Gogate et al., 2001a). This also stresses the point of using higher dissipation areas for obtaining better cavitational results.

Measurement of local pressure

As was said earlier, the local pressure amplitudes were measured using a hydrophone (Bruel & Kjaer Ltd., Type 8103, Denmark), and a charge amplifier. The dimensions of the hydrophone used were: length, 50 mm, and diameter, 9.5 mm. The hydrophone was always protected against cavitation by a rubber sheath. The calibration curves supplied by the manufacturer takes into account the absorption coefficient of this rubber sheath, so no errors will be introduced due to this protection. The values of intensity calculated with the help of

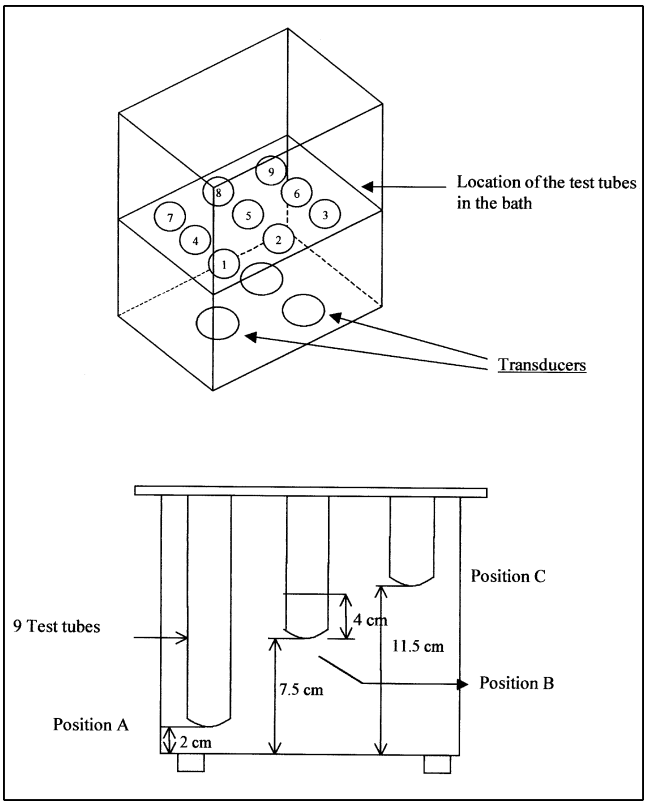

Figure 1. Location of the test tubes and the transducers in the ultrasonic bath.

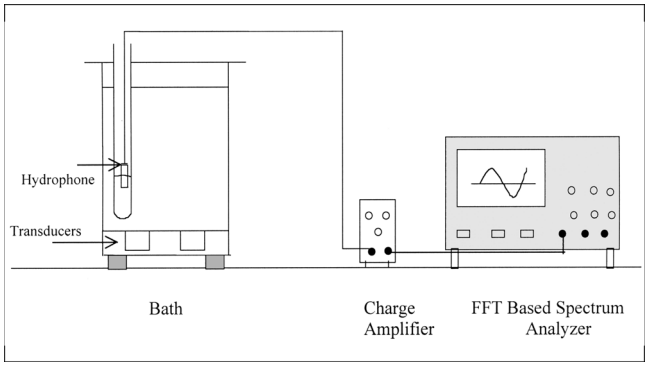

Figure 2. Experimental setup used for acoustic mapping in the ultrasonic bath.

pressure measurements using a hydrophone were compared with those estimated on the basis of energy dissipated into the liquid medium under experimental conditions, and a good agreement was observed between the two.

Water was taken in the bath as a cavitating medium and was filled up to a height of 15 cm. The measurements were carried out at nine different locations, as indicated in the Figure 1, facilitating the studies for the axial as well as radial variation of the cavitational activity. The three different locations along the height of the bath were chosen as a function of the wavelength of the ultrasound (position A was at a distance of $\lambda/4$, whereas positions B and C were at distances λ and $3\lambda/2$, respectively from the bottom of the bath). The positions in the radial direction were such that one of the positions was in the center of the bath (also the center of the triangle marked by the transducers at each of its apexes), while the other two positions were equidistant from the axis passing through the center and nearer to the wall. Twenty mL of water (height of water in the glass test tubes = 4 cm) was put in each of the test tubes (ID = 25.3 mm; OD = 28.6 mm; length = 150 mm) and the hydrophone was then suspended in it. The signal from the hydrophone was amplified through a charge amplifier and fed to a fast Fourier transform (FFT) based spectrum analyzer (Lecroy Ltd., Model 9310 M, USA). Figure 2 shows the experimental setup used in the present work. The resultant output was recorded in terms of mV for the corresponding frequencies. From the FFT, it was observed that peaks were obtained at the driving frequency, multiples of the driving frequency (that is, at 40, 60 and 80 kHz), and subharmonics (10 kHz). Using the hydrophone calibration details supplied by the manufacturer, the amplitudes of the pressures were calculated at these peaks. As cavitation is a very random phenomenon, two consecutive readings at the same conditions may yield completely different results in terms of the measured pressure amplitudes. Therefore, 60 pressure pulses were collected for a particular frequency at a particular location in the bath. The same procedure was then repeated for the remaining eight different positions and at three different heights. The 60 readings ensured that a statistically significant number of samples were measured, which reduces the random variation in the measured pressure pulse due to the occasional cavity collapse.

A similar procedure was also adapted for measurements in the case of the ultrasonic horn. The measurements were made in the axial direction, with increasing distance from the tip of the horn, and also some measurements were made in the horn-tip plane in the radial direction. The experimental setup used is shown in the Figure 3.

Measurement of chemical effects

As explained earlier, it is very important to know how this variation in the local pressure affects the reaction rates for any chemical system. The model reaction considered in the present work is a decomposition of potassium iodide, which frees iodine (in the absence of CCl_4). It should be noted at this stage that this reaction is only induced due to the cavitation and not by shear temperature and pressures (Suslick et al., 1997; Senthilkumar et al., 2000). This is due to the fact that free OH· radicals are formed in the solution only under cavitating conditions. These free radicals then attack KI liberating iodine. Details of the chemical reaction and quantification of liberated iodine were discussed earlier (Gogate et al., 2001a).

In this work, variation in the pressure intensities and KI decomposition rates were studied at the same location, but with nine glass test tubes of apparently similar dimensions. These measurements were also repeated by using a single glass test tube at different locations to check if the variation in the thickness and curvature of the glass test tubes had any effects on the cavitational fields at that location. The time of irradiation was fixed at 20 min. The same procedure was repeated at all the locations using the same test tube. The need for the use of the single test tube is discussed in detail later.

Bubble-dynamics studies

As said earlier, it is important to link the measured driving pressure fields with the observed chemical effects and obtain a relationship between them. The driving pressure is responsible for the cavitation phenomena where the generated cavities expand to a maximum cavity size and then undergo violent collapse, generating a large magnitude of the pressure pulse and the temperatures responsible for the observed chemical effects. The magnitude of the cavity collapse pressure is dependent on the maximum size of the cavity and also on the time taken for the collapse.

In the acoustic cavitation, the most important parameter affecting the bubble dynamics other than the frequency of the ultrasound is the operating intensity of the irradiation. Ultrasound intensity is directly related to the pressure amplitude, and is given by the following equation

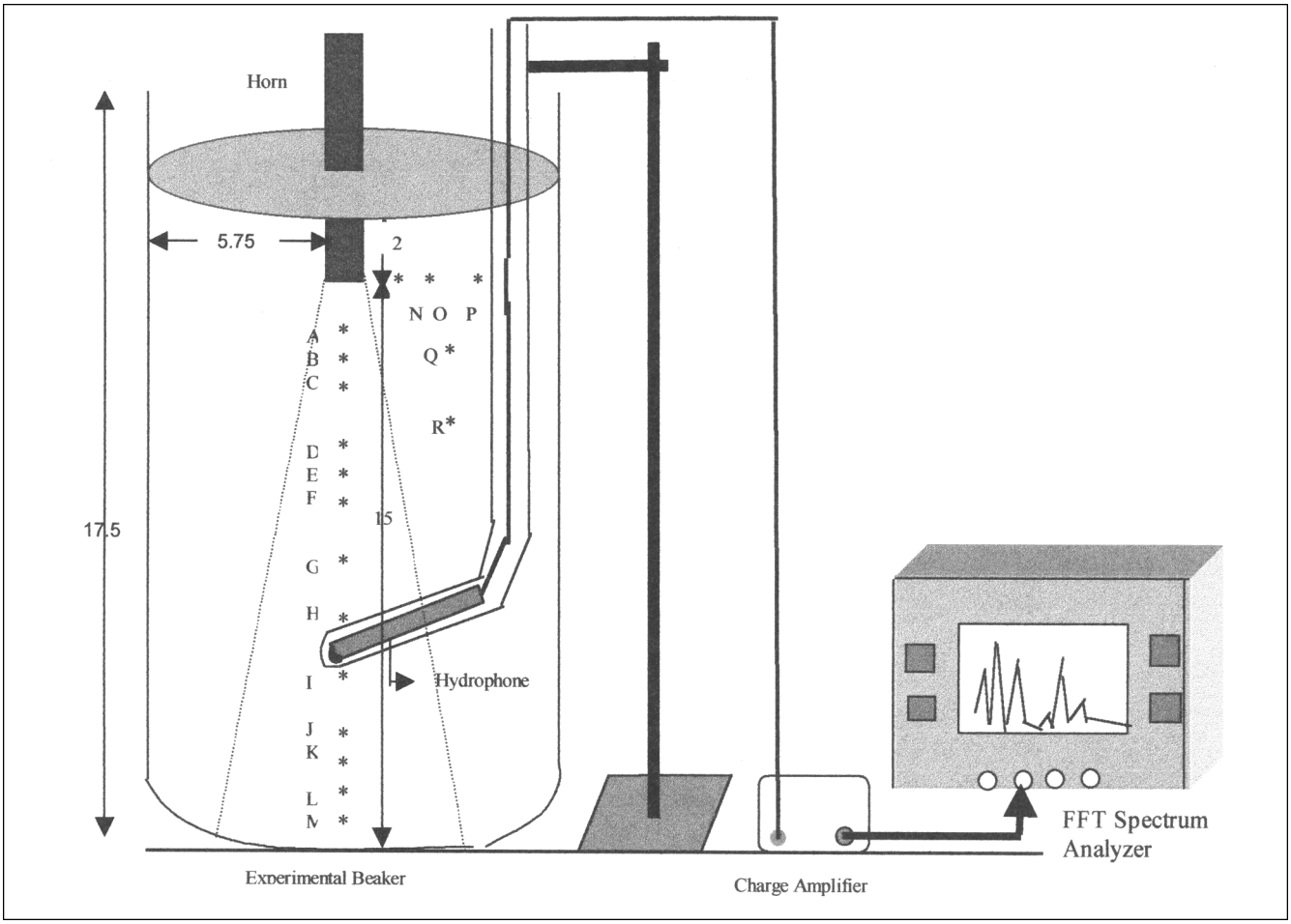

Figure 3. Experimental setup used for acoustic mapping in the ultrasonic horn.

$$P_A = \sqrt{2I\rho C} \tag{1}$$

where P_A is the driving pressure amplitude, I is the intensity of irradiation, ρ is the density of the liquid medium, and C is the velocity of sound in the medium.

Simulations were carried out to discover how the variation in the local pressure amplitude affects the bubble dynamics. The measured values of the pressure amplitude were substituted for P_A in the equation for the local fluctuating component of pressure given below

$$P_\infty = P_o - P_A[\sin(2\pi ft)] \tag{2}$$

where f is the frequency of irradiation (20 kHz) and P_o is the initial pressure inside the bubble.

The radial wall motion of the bubble was well described by the bubble dynamics equation developed by Rayleigh and later modified by Plesset (1949), more commonly known as the Rayleigh–Plesset equation. It was shown in the previous work (Gogate and Pandit, 2000) that the assumption of the incompressible nature of the liquid in this equation severely underestimates the magnitudes of the generated cavity collapse pressures. A rigorous and more realistic equation for considering the compressible nature of the liquid medium was used for numerical simulations in the present case. Details on the simulation conditions, the solution methodology, and the assumptions involved in these equations were described in the earlier work (Gogate and Pandit, 2000), and so are not repeated here. To give readers a feel of the rigorous nature of the equation, it has been depicted here as follows:

$$R\ddot{R}\left(1-\frac{2\dot{R}}{C}+\frac{23\dot{R}^2}{10C^2}\right)+\frac{3}{2}\ddot{R}^2\left(1-\frac{4\dot{R}}{3C}+\frac{7\dot{R}^2}{5C^2}\right)$$
$$+\frac{1}{\rho l}\left[\begin{array}{l} p_\infty(t)-p_{2(r=R)}+\dfrac{R}{C}\left(\dot{p}_\infty(t)-\dot{p}_{1(r=R)}\right) \\ +\dfrac{1}{C^2}\left\langle\begin{array}{l} -2R\dot{R}\left(\dot{p}_{\infty(t)}-\dot{p}_{1(r=R)}\right)+\dfrac{1}{2}\left(p_{\infty(t)}\right. \\ \left.-p_{1(r=R)}\right)\left(\dot{R}^2+\dfrac{3}{\rho_l}\left(p_{\infty(t)}-p_{1(r=R)}\right)\right)\end{array}\right\rangle\end{array}\right]=0 \tag{3}$$

where the P_1 and P_2 as a function of R are given as follows

$$p_{1(r=R)} = p_v - p_{go}\left(\frac{R_0}{R}\right)^{3\gamma} - \frac{2\sigma}{R} - \frac{4\mu}{R}\dot{R} \tag{4}$$

$$p_{2(r=R)} = p_{1(r=R)} - \frac{4\mu}{3\rho C^2}\left(\dot{p}_{\infty(t)} - \dot{p}_{1(r=R)}\right) \tag{5}$$

The various parameters involved in the equation are given in the Notation section. The simulations were performed for the peak frequency as observed in the Fourier frequency transform and for an initial cavity size of 2 μm. It has been generally observed that the cavity sizes produced in the case of sonochemical reactors are of the order of a few microns (typically in the range 1–10 microns), though recent experimental investigations (Tsochatzidis et al., 2001) have indicated a cavity size of 10 μm as the minimum. It should be noted that the cavity size depends largely on the type of the equipment and the operating conditions (intensity and frequency of irradiation), along with the physicochemical properties of the liquid medium. The selection of the 2-μm cavity size was only as a representative value in the range generally observed. Further research has to investigate the effect of cavity size on the cavitational yields, as well, and the generalized correlation should also consider this effect.

For each value of the driving pressure, the maximum radius reached by the growing bubble during the growth stage of the cavitation phenomena was obtained from the solution of the bubble dynamics equation. The maximum bubble radius gives an indication of the nature of cavitation, that is, stable or transient, and hence the final pressure/temperature pulse that is likely to be generated that results in the desired effects.

Results and Discussion

Effect of the test tube of similar dimensions

A major point in the experimental investigations into different aspects of sonochemistry is the reproducibility of the results obtained, which is relatively easy to obtain within a laboratory because of internal consistency. It is somewhat more difficult to obtain between different laboratories for the same sets of conditions. Minor changes in the experimental conditions lead to different results and so a careful scrutiny and a characterization of the equipment to be used should be carried out first. Luche (1999) has discussed the variation in the chemical yield due to change in the vessel geometry. Pugin (1987) has reported higher intensities in flat-bottom flasks than in round bottom flasks.

To characterize the different test tubes used in the investigation, experiments were conducted with different test tubes at a single predefined location (1 A, as per the Figure 1). The volume of KI solution taken was also kept the same in all the test tubes, which were of the same diameter. The results obtained are depicted in Figure 4. It can be seen that although

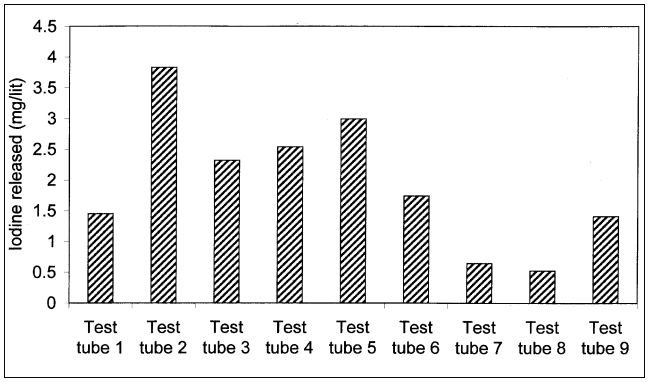

Figure 4. Variation of the amount of iodine released at the same location with type of the test tube.

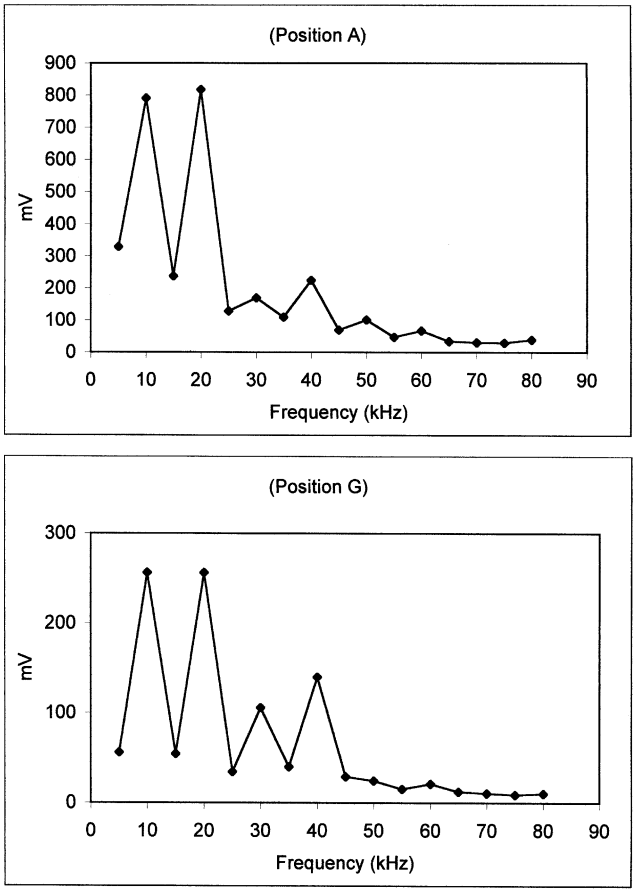

Figure 5. Frequency Fourier transform (FFT) curves for two different positions in the case of the ultrasonic horn.

the location is the same, which means that the time-averaged local ultrasonic activity will be the same, there is wide variation (up to eight times between the maximum and minimum iodine liberations) in the amount of iodine liberated over a constant period of 20 min. It should be noted at this stage that the readings of freed iodine are the average of three runs and the variation in these three readings is within $\pm 10\%$, which can be attributed to the randomness of cavitational events and experimental inaccuracies. Thus, the observed variation can be attributed to the difference in the curvature of the test tubes and the thickness of the glass tube, which attenuates the ultrasound to a different extent, resulting in a variation in the local pressure amplitudes, and thus affecting the cavitational activity and the KI decomposition rates. This point is quite critical, as while doing experiments, one is always satisfied with the global matching of the instruments used in the investigations and the microvariations are usually not considered. So it can be said that for various laboratories working on the same sets of conditions, the results can vary by nearly 10 times due to the changes in the thickness and/or curvature of the test tubes, resulting in a variation in the degree of attenuation of the various frequency waves in the secondary equipment used (such as test tubes, beakers, and so on).

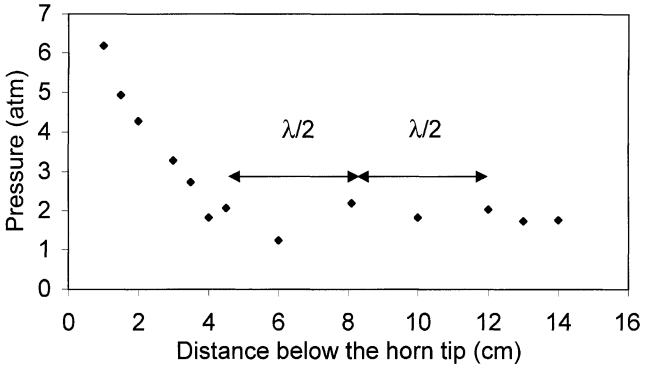

Figure 6. Variation of the ultrasonic activity in the axial direction for the ultrasonic horn.

This point also needs to be considered where microreactors are used at strategic positions with the most ultrasonic activity, as predicted by the numerical simulations for enhanced cavitational yield from the reactor. Optimization needs to be carried out, and the selection of these microreactors should be for maximum global benefits.

Variation in the local intensity

Ultrasonic Horn. The FFT response curves for two sample positions, viz., at a distance of 1 cm from the tip of the horn (A), and at distance 4.5 cm away from the tip (G) are shown in Figure 5. The figure shows that peaks are observed at the driving frequency (20 kHz) as well as at multiples of the driving frequency (that is, 40 kHz, 60 kHz, and 80 kHz). Moholkar et al. (2000) have shown that these peaks are absent for the noncavitating liquids. Noncavitating liquids show only one peak at the driving frequency. This is because, in the case of water, the acoustic emission spectra are composed of ultrasound waves with the pressure pulses caused by bubble oscillation/collapse superimposed on it. However, for noncavitating liquids such as silicon oil (with viscosity on the order of 200 CP), cavitation phenomena are not seen to result in only the fundamental frequency peak. The figure also shows that the intensity of the peak at the driving fundamental frequency is greater for position A compared to position G. This is in accordance with many earlier studies on mapping the ultrasonic horn (Chivate and Pandit, 1995; Romdhane et al., 1995a, Romdhane et al., 1997).

A complete profile for the variation of the local ultrasonic activity with axial distance from the horn tip is shown in Figure 6. The trend observed is again similar to the earlier observations of decreasing activity as the distance increases. Moreover, it also can be seen that the ultrasonic activity shows intermediate peaks, that is, an increase in the intensity with the distance between two peaks approximately equal to $\lambda/2$. Pugin (1987) and Romdhane et al. (1995a, 1997) have obtained similar results. The intermediate increase in the local ultrasonic activity can be attributed to the prominent subharmonic peaks (observed at frequency = 10 kHz) at these locations. The FFT response at position G (distance = 4.5 cm) shows a dominant peak in pressure intensity at frequency of 10 kHz, which is equal to $f/2$, where f is the driving frequency for the horn (see Figure 5). Such a peak was not observed at the earlier location, F, at a distance of 4 cm from

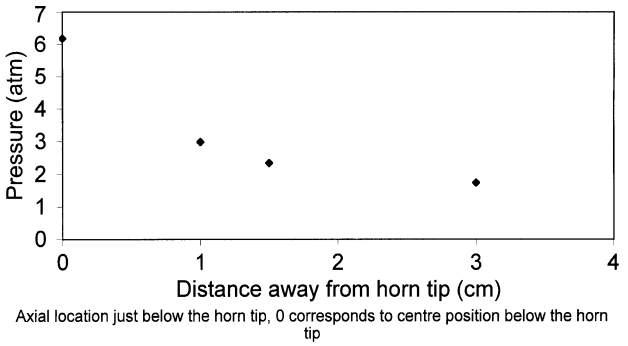

Figure 7. Variation of the ultrasonic activity in the radial direction for the ultrasonic horn.

the tip of the horn. Esche (1952) has shown that subharmonically oscillating bubbles evolve into transient cavities. Transient cavitation is more efficient and results in a relatively more violent collapse of cavities compared to stable cavitation, resulting in higher local pressure as well as iodine liberation at these locations.

Experiments were also performed at different radial locations to check for the radial homogeneity of the ultrasonic activity. The results are shown in Figure 7. It easily can be seen from the figure that the ultrasonic intensity measured in terms of local pressure decreases with an increase in the distance from the axis passing through the center of the irradiating surface. The observed results are in agreement with the results obtained by Romdhane et al. (1995a), who have shown that the ultrasonic activity diminishes at a distance of 3 cm from the center axis.

At all these locations, experiments were repeated using KI decomposition as the model reaction. A one-to-one correspondence was observed between the measured pressure amplitudes using the hydrophone and the rates of iodine liberation. The trends obtained with both sensors were similar, indicating that the type of method used for the mapping of ultrasonic reactors does not play a major role in the results. Faid et al. (1998) have also obtained the same results using different sensors. Details of the dependency of KI decomposition rates on the driving measured pressure fields are discussed later.

The observed results once again conclusively establish that the ultrasonic activity is maximum at the zone very close to the irradiating surface and decreases as one moves away from the source both in the axial and radial direction.

Ultrasonic Bath. For the ultrasonic bath-type reactor, the experimental measurements were carried out at different locations with variations in the radial as well as axial directions in the reactor. The test tube was placed in the bath at three different heights, as shown in Figure 1. The FFT response for the three different heights for the same radial location 1 in the bath is shown in the Figure 8. The trend of the peaks at the harmonics (Frequency = multiples of driving frequency, 20 kHz) and subharmonics (driving frequency/2) is similar to that obtained for the ultrasonic horn, which confirms the presence of cavitating bubbles in the reactor, as discussed earlier. The figure also shows that for position 1A the pressure amplitude (given in terms of the measured values in mV) at the driving frequency is maximum, and the

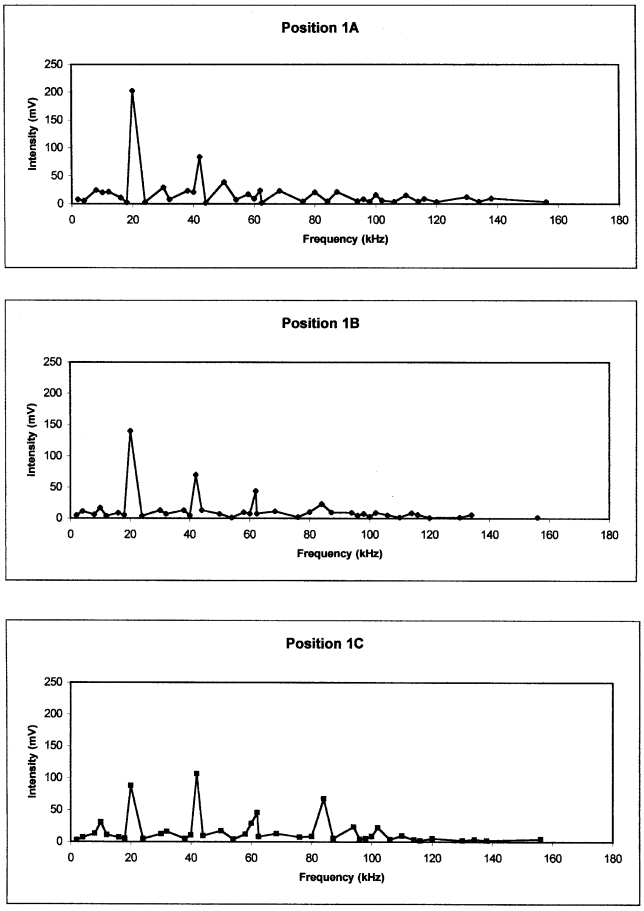

Figure 8. Frequency Fourier transform (FFT) curves for different positions in the case of the ultrasonic bath.

amplitude decreases as we move from the bottom of the bath to position 1B and 1C. It should be noted that position 1 is located on the side of a single transducer and at the extreme radial position, and hence will be under the maximum influence of only that particular transducer. Contamine et al. (1994) have also reported a decreasing mass-transfer coefficient at a distance from the bottom of the tank, indicating decreased ultrasonic activity. Soudagar and Samant (1995), with the help of experimental measurements using a PPIMP transducer, and Dahnke et al. (1999a,b), with the help of theoretical modeling of pressure fields, have obtained similar trends.

At the center of the bath, that is, at position 5 (see Figure 1), the exact opposite trend is observed. The pressure amplitude for the position 5B is higher as compared to that at position 5A and 5C, which contradicts the results obtained from the other positions. The observed result can be attributed to the transducer arrangement at the bottom of the bath (triangular pitch), and hence the maximum-intensity acoustic field is formed at the center position compared to the other locations in the bath. Soudagar and Samant (1995) have also found that for three transducers, arranged to form an equilateral triangle at the base of the bath, the pressure amplitude is maximum at the center of the triangle at the

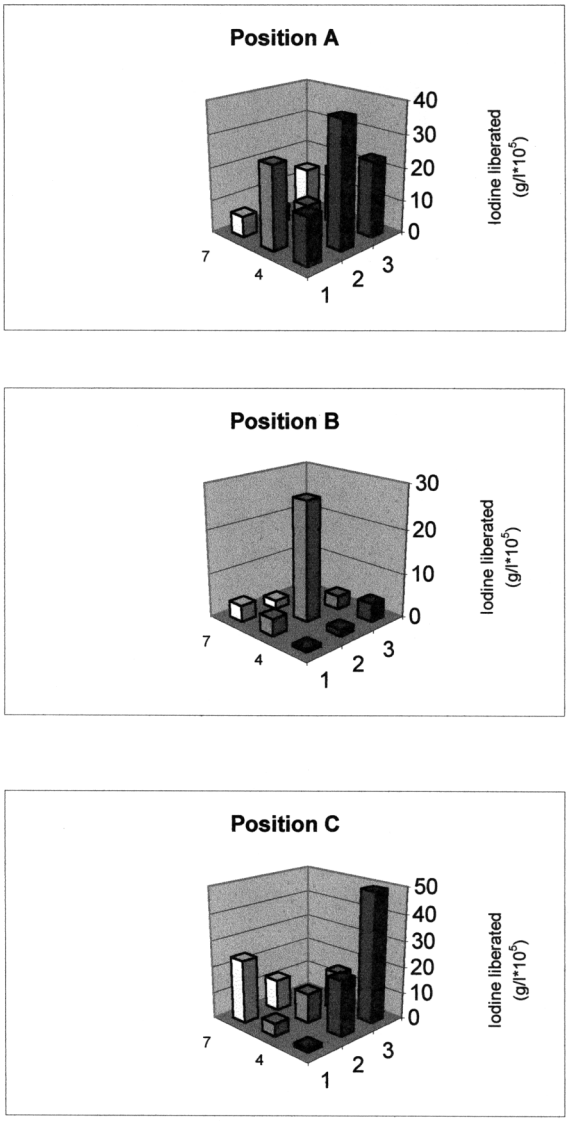

Figure 9. Variation in the iodine yield with location for various positions in the ultrasonic bath.

λ-plane (the axial distance of the horizontal plane from the bottom of the tank is equal to the wavelength of the driving sound source) and minimum exactly above the transducers at the same horizontal plane. This opens up a new field for further research. The locations of the multiple transducers can be adjusted so as to get multiple locations where the intensity would be high, thereby increasing the global cavitational yields from the sonochemical reactors.

The extent of iodine liberation at the various locations in the ultrasonic bath are depicted in Figure 9. The variation in the iodine liberation rates at these positions for the ultrasonic bath was again similar to the variation in the measurements in the local pressure amplitudes, confirming the one-to-one correspondence between the two, except for location 3C, which is in the zone of influence of the two transducers. Again, details of the relationship between the two are discussed later in the article.

Thus, it can be said that for the ultrasonic bath, the ultrasonic activity is uniform in neither the horizontal plane nor the vertical plane. The formation of standing-wave patterns resulting from the reflections of the ultrasound from the reactor wall and also from the air–water interface may be one of the reasons for the observed nonuniformity. Standing waves are two waves acting in the opposite direction, such that the particle's net displacement from its mean position is zero at the node and maximum at the antinode, due to the influence of the second wave.

The bubble behavior in the standing waves can be explained with the help of Bjerknes forces. Small bubbles or cavities are driven into the antinodes of the pressure and large bubbles are driven into the pressure nodes (Eller and Flynn, 1969). This can be verified in the present case by analyzing the FFT curve for position C (Figure 8). Antinodes are formed at position C, as it is $3\lambda/2$ from the bottom of the bath. The presence of the higher frequency peaks confirms the existence of smaller bubbles (with higher resonant frequency) at this position. The smaller cavities result in transient cavitation, whereas larger cavities result in stable cavitation. These smaller cavities, which are driven into the pressure antinodes, grow larger, as the pressure amplitude is higher in these zones, resulting in higher cavitational activity. Thus, even though the pressure amplitude at the driving frequency is lower compared to that at positions nearer to the bottom of the tank, the contribution of the peaks observed at harmonics and the effect of standing waves results in higher cavitational yields at these locations (Figure 9).

Quantification of iodine yield in terms of measured pressure amplitude

Ultrasonic Horn. Figure 10 shows the variation in the amount of iodine freed with the measured pressure amplitude in the ultrasonic-horn reactor. It easily can be seen that a linear relationship exists between the two given by the following equation, which is obtained by a curve-fitting exercise with an R^2 value of 0.933 indicating good fit

$$\text{Iodine yield} = (9.816\times10^{-6})\ \text{pressure amplitude} - 3.235\times10^{-6} \quad (6)$$

It should be noted that the points that show an increase in iodine liberation at distances of $\lambda/2$ in the axial direction due to the contributions of subharmonic and harmonic pressure amplitudes have not been considered in the curve-fitting exercise. A quick analysis of the equation reveals that the threshold pressure required for the start of iodine liberation, that is, the positive effects of cavitation phenomena, is equal to 0.33 atm. The existence of threshold pressure for iodine liberation can be explained on the basis of the mechanism of the decomposition of KI.

Naidu et al. (1994) have explained the mechanism of the decomposition of KI. Upon sonication, water molecules are pyrolyzed to form hydrogen and hydroxyl radicals. These radicals then oxidize potassium iodide to give iodine. Hence, the liberation of iodine is directly proportional to the formation of hydroxyl radicals. The radicals are generated only when the conditions are favorable for the pyrolysis of water. This can occur only above a specific threshold pressure inside the

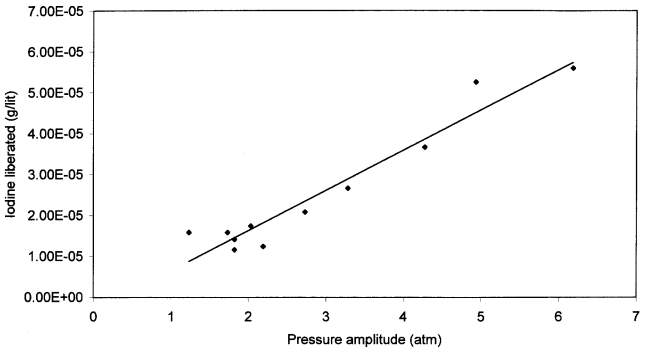

Figure 10. Variation of iodine yield with measured pressure pulse for the ultrasonic horn.

collapsing cavities, which indicates the existence of a threshold pressure for the decomposition of KI. Beyond this threshold, the amount of iodine liberated increases linearly with an increase in the driving pressure, which will also influence the cavity collapse pressure once the threshold pressure is exceeded.

Ultrasonic Bath. Figure 11 shows the variation in the amount of iodine liberated with the measured pressure amplitude in the ultrasonic-bath reactor. The trend of the variation is similar to that obtained for the ultrasonic-horn reactor, with linear variation between the two and the existence of a threshold value for pressure amplitude. The curve-fitting exercise gives the following equation for the variation with an R^2 value of 0.89 and threshold pressure for the onset of the liberation of iodine of 2.57 atm

$$\text{Iodine yield} = (4.053\times10^{-4})\ \text{pressure amplitude} - 1.048\times10^{-3} \quad (7)$$

It can be seen that the constants for the linear variation of the pressure amplitude are higher for an ultrasonic bath reactor, indicating that the same driving-pressure amplitude is better transformed into secondary effects, that is, liberation of iodine. Thus, ultrasonic-bath reactors are more efficient for cavitational applications as analyzed by experiments with the model reaction. In some earlier works (Gogate et al., 2001a,b), similar results were obtained; these were also discussed in detail in the earlier sections of this article. It also can be seen that the threshold pressure required for the onset of cavitational effects in the case of an ultrasonic bath reactor is greater compared to an ultrasonic horn reactor, a fact that needs to be considered for the selection of particular equipment, but is still far from understood. The observed experimental result may be attributed to the diffused energy effect in the case of the ultrasonic bath, whereas greater concentrated energy will be available in the ultrasonic horn (almost 15 times lower power dissipation per unit volume in the case of the ultrasonic bath compared to the horn).

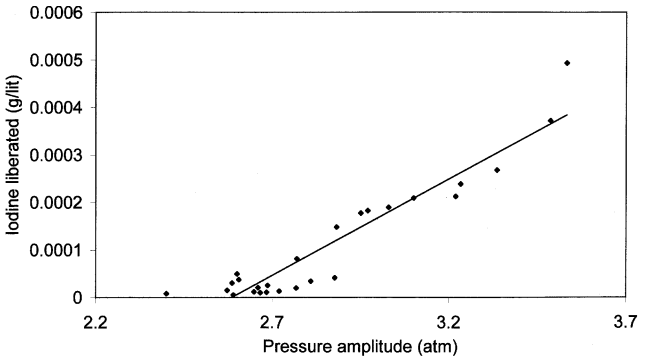

Figure 11. Variation of iodine yield with measured pressure pulse for the ultrasonic bath.

The quantification exercise explains the correspondence between the measured pressure amplitudes and the iodine liberation rates, and also conclusively proves the enhanced efficacy of the ultrasonic-bath-type reactors. It also should be noted that these measured pressure values do not give a correct picture, as they are extremely low compared to the actual values, and hence the equations given earlier should be considered only for establishing the trends. More realistic equations can be developed in terms of either the collapse pressure or the maximum radius reached during the expansion phase of the cavitation phenomena, as explained in the following subsection.

Variation of iodine yield with maximum bubble size

As explained earlier, the values of measured pressure pulses at the driving frequency were used in the bubble-dynamics simulations for estimating the maximum bubble size reached during the cavitation, and also for quantification of the pressure pulse that will be generated at the end of the cavitation event. The value of the estimated pressure pulse corresponds to the collapse of the single cavity, whereas the maximum radius gives us an indication of the number of free radicals released in the solution due to the collapse of the cavities. The estimation of these quantities is necessary, as the measured pressure pulses do not correspond to the actual values; in fact, they are lower, and the maximum radius confirms the type of cavitation taking place, that is, whether transient or stable.

The pressure pulses arising from the transient collapse of an individual bubble undergo large attenuation due to absorption by the bubble cloud surrounding the collapsing bubble and the nonlinearities of the medium. Matula et al. (1998), using a generalized form of Burger's equation, have estimated the attenuation of the pressure pulse for bubbles to be greater than 5 μm. If we assume that the pressure pulses resulting from the transient collapse of the bubbles are affected by spherical spreading, calculations show that the measured amplitude of the pressure pulse is almost 1,000 times lower than its actual value at a distance as low as 1 mm from the center of the bubble generating the pressure pulse. Therefore, there is a large difference between the magnitude of the pressure pulses theoretically estimated at the collapsing cavity wall and those actually measured using any dynamic pressure transducer. Also, in the present case, a similar trend has been observed. While the measured pressure pulses are on the order of a few atmospheres, the ones calculated using numerical simulations were on the order of 10^6 atmospheres for an assumed initial cavity size of 2 μm.

The simulated values of maximum bubble size give an indication of the type of cavitation taking place at the different locations. Cavitation bubbles are classified as stable or transient, according to their radial motion as influenced by the acoustic field. Flynn (1975) has characterized the stable and transient cavities as follows: if the ratio of R_{max}/R_o during the radial motion exceeds the minimum value given by (7.48 $P_{go}/P_o)^{1/3}$, the resulting cavitation will be transient. For air bubbles in water, this ratio is found to be equal to 2. In this work, numerical simulations result in an R_{max}/R_o ratio of greater than 2 for all the measured pressure amplitudes, indicating the occurrence of transient cavitation at all the considered locations, which is also confirmed by the release of a measurable amount of iodine. It also should be noted that in the case of stable cavitation, the cavities just oscillate without releasing a significant amount of energy, and hence the chemical reactions do not occur.

The variation in the amount of iodine liberated with the maximum radius $[(R_{max}/R_o)]^3$ is considered, as the volume of the collapsing bubble is relative to the amount of the free radicals released into the reactor] is shown in Figure 12. It is easily seen that iodine liberation varies linearly with the ratio corresponding to the volume of the bubble, indicating that the generation of the free radicals is the rate-controlling step, and the presence of the X intercept indicates that a certain minimum concentration of free radicals is always required for the chemical reaction to occur. The mathematical equation relating the two as obtained by the curve-fitting exercise with an R^2 value of 0.94, is given below

$$\text{Amount of iodine liberated} = 8.562\times10^{-6}\,(R_{max}/R_o)^3 - 3.847\times10^{-4} \quad (8)$$

The preceding equation also can be modified by using a specific gas constant, that is, using term $(R_{max}/R_o)^{3\gamma}$ instead of $(R_{max}/R_o)^3$, as the magnitude of the collapse pressure pulses can be directly estimated as a function of $(R_{max}/R_o)^{3\gamma}$ (Young, 1989). The new equation with an R^2 value of 0.94 is given below

$$\text{Amount of iodine liberated} = 1.14\times10^{-6}\,(R_{max}/R_o)^{3\gamma} - 2.3\times10^{-4} \quad (9)$$

Thus, the rate of iodine liberation will be higher at higher R_{max} values, which in turn depend on the measured pressure amplitude (direct variation has been observed). Thus, for higher local power dissipation, that is, higher ultrasound dissipation intensities, the amount of iodine liberated will be higher. Entezari and Kruus (1996) have investigated the effect of the increase in intensity (and hence, the pressure amplitude) on the reaction rates of decomposition of KI and reported an increase in these rates when there is an increase in the power dissipated. Although, the observations of Entezari and Kruus (1996) are based on the global rates, the comparison is just to indicate the correctness of the trend observed in our measurements. However, the increased power dissipation results in an increase in the iodine liberation only until a certain power dissipation rate corresponding to the optimum intensity, which was mentioned earlier and was also discussed in details in an earlier work (Gogate et al., 2001a). The reason for this can be attributed to the decrease in the collapse pressures as obtained by the numerical simulations when the intensity of irradiation is increased (Gogate and Pandit, 2000). In the present work, $(R_{max}/R_o)^3$ has been used as the correlating parameter for the iodine yield, as the number of free radicals generated is the rate-controlling step once the operating pressure exceeds the threshold pressure. In an earlier work (Gogate et al., 2001a), the correlating parameter used was the overall pressure pulse generated at the collapse of the cavities, as the data were based on the wide range of operating parameters, which included variations in both operating frequency and intensity of irradiation. Nevertheless, maximum size also gives an indication of the maximum collapse pressure likely to be generated, though not the absolute value, and hence can be used as a correlating parameter.

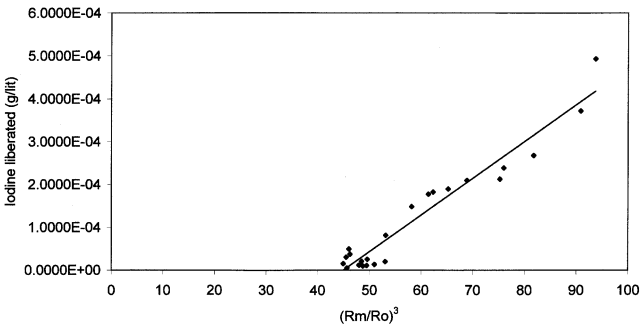

Figure 12. Variation of the iodine yield with maximum bubble size as obtained from numerical simulations.

The constants obtained in the equation depend on both the type of the equipment and the operating parameters. This is because $(R_{max}/R_o)^3$ gives an indication of the extent of the free radicals generated theoretically, whereas the iodine liberated was calculated from the experimental measurements. All the free radicals generated in the bubble may not be available for the chemical reaction; it depends on the type of the mechanism that destroys the bubble. In the case of multibubble situations, if the bubbles are unstable on collapse and break apart, in some way dispersing their total OH· content into the liquid (Colussi et al., 1998), a peak number of radicals will be available for the sonochemical reactions. However, if the breakup bubbles are stable and the OH· radicals enter the liquid by uptake across the interface, the number of radicals available will be substantially lower. Storey and Szeri (2001) have indicated an uptake coefficient of 0.001, which means that only 0.1% radicals are available for the chemical reactions to occur. The type of bubble collapse will necessarily depend on the equipment used for generating the cavitation and the operating conditions. Takami et al. (1998) have also focused on the concept of the uptake coefficient for the free radicals on an aqueous surface.

It should be noted that the developed correlation, unique of its kind, along with the earlier correlation of cavitational yield in terms of developed collapse pressure (Gogate et al., 2001a) are only trend setting and are by no means a general one. There is ample scope for further work, which could in-

clude establishing the validity of the equations over a wider range of operating parameters, exactly quantifying the number of free radicals generated during the collapse (more importantly estimating the actual number taking part in the reaction, by considering the number of free radicals generated, time of collapse of the cavities, and the lifetime of the free radical), estimating the size of the nuclei/cavity that will be strongly dependent on the type of equipment used for the generation of cavitation, combining the effects of collapse pressure generated, and the maximum bubble size reached. Studies in this direction are also being carried out in this department. Some recent works (Rajan et al., 1998a,b; Sochard et al., 1998; Storey and Szeri, 1999, 2000; Moss et al., 1999; and Tsochatzidis et al., 2001), can also serve as useful guidelines for establishing the generalized correlation considering the preceding facts.

Conclusions

The nature of the sound/cavitational field existing in any ultrasonic reactor is substantially nonuniform, with spatial variations in the axial as well as radial directions. In general the activity shows a decreasing trend away from the transducer and is maximum in the vertical plane of the emitting area. The type of the sensor used (hydrophone for pressure measurements and chemical source for measuring rates of chemical reaction) for mapping the local field does not affect the trends observed, and one-to-one correspondence is observed between the two.

Reactors with a higher area of irradiation are better; in the present case, the ultrasonic-bath reactor results in larger amounts of iodine liberated as compared with the ultrasonic-horn reactor, on the basis of unit energy consumption. Higher proportionality with respect to the measured pressure pulses also conclusively establishes that the same pressure pulse will be better utilized for the desired effects in the case of the ultrasonic bath reactor.

The existence of a threshold pressure pulse or limiting value of the number of the free radicals [indicated by a limiting value of $(R_{max}/R_o)^3$] is established conclusively by the quantification of iodine liberation in terms of measured pressure pulse and the maximum cavity growth predicted by the numerical simulations.

Detailed analysis of the existing literature points toward the need for developing new sonochemical reactor designs by using multiple transducers, located in different positions (such as parallel to each other, in a triangular pitch at the bottom, and a hexagonal design with transducers on each face of the hexagon) in order to achieve the uniform distribution of energy. In addition to multiple transducers, multiple frequency operation also facilitates the uniform distribution of energy, and may lead to minimal erosion rates in the transducers. Multiple-frequency operations offer more flexibility compared to conventional single-frequency reactors. The radially vibrating horn is also a new concept, as to a large extent, it eliminates nonuniformity in the radial direction and also has some activity in the longitudinal direction. New designs facilitating the continuous operation of the acoustic-cavitation-based reactors is also a daunting future task for researchers.

The simultaneous effects of the flow regimes on the cases of the recirculating type of reactor, speed of agitation, and the presence of solids (size of each solid and its concentration) in terms of enhancing the reaction rates, on the one hand, and disturbing the sound field resulting in lower ultrasonic activity, on the other hand, is another major factor that needs to be considered in the rational design procedure. The standing waves have been reported to enhance the global sonochemical yields, but the exact role of standing waves is still not understood.

More studies are also required to conclusively link the values of the pressure pulse at different locations, obtained using numerical simulations [the work of Keil and coworkers is recommended for this, as discussed earlier (please refer to Table 1 for the details)], with the observed chemical effects using different chemical reactions. The correlation developed in the present work is only a first step, so more work is required in the areas of predicting the number of free radicals generated, the exact quantification of the collapsed temperatures and pressures as a function of distance in the cavity, the lifetime of the cavity, and estimation of cavity size, and relating these important parameters to the cavitational yield before a generalized correlation for the prediction of cavitational yield as a direct function of the operating parameters can be developed. Such generalized correlations will be very helpful in the effective design and scale-up of the sonochemical reactors.

Acknowledgment

The authors acknowledge the funding of the Indo-French Center for the Promotion of Advanced Research (Centre Franco-Indien Pour La Promotion de La Recherche Avancee), New Delhi, India, for the collaborative research work.

Notation

C = velocity of sound in the medium, m/s
f = frequency of ultrasound, kHz
I = intensity of irradiation, W/m^2
P_o = initial pressure inside the bubble, N/m^2
p_{go} = initial gas pressure in the bubble, N/m^2
P_A = driving pressure amplitude, N/m^2
P_{max} = maximum electric power supplied to the equipment, W
p_v = vapor pressure, N/m^2
P_∞ = pressure in the surrounding liquid, N/m^2
P_1, P_2 = initial and final pressures during each simulation step, respectively, N/m^2
$P = (dP/dt)$, rate of change of pressure with time, N/m$^2\cdot$s
r = radial distance from the bubble wall, m
R = radius of cavity/bubble, m
R_{max} = maximum radius of the bubble/cavity, m
R_o = initial radius of the bubble/cavity, m
$\dot{R} = (dR/dt)$, bubble wall velocity, m/s
$\ddot{R} = (d^2R/dt^2)$, bubble wall acceleration, m/s^2
t = time

Greek letters

γ = specific gas constant
λ = wavelength of the ultrasound, m
ρ, ρ_l = density of the liquid medium, kg/m^3
μ = viscosity of liquid, Ns/m^2
σ = surface tension of liquid, N/m

Literature Cited

Ambulgekar, P. V., A. C. Dedhia, and A. B. Pandit, "Drainage of Liquid in Static Foam: Role of Ultrasound," *Chem. Eng.*, in press (2002).

Bhatnagar, A., and H. M. Cheung, "Sonochemical Destruction of Chlorinated C1 and C2 Volatile Compounds in Dilute Aqueous solutions," *Environ. Sci. Technol.*, **28**, 1481 (1994).
Cheung, H. M., A. Bhatnagar, and G. Jansen, "Sonochemical Destruction of Chlorinated Hydrocarbons in Diluted Aqueous Solutions," *Environ. Sci. Technol.*, **25**, 1510 (1991).
Chivate, M. M., and A. B. Pandit, "Quantification of Cavitation Intensity in Fluid Bulk," *Ultrason. Sonochem.*, **2**(1), S19 (1995).
Colussi, A. J., L. K. Weavers, and M. R. Hoffmann, "Chemical Bubble Dynamics and Quantitative Sonochemistry," *J. Phys. Chem. A*, **102**, 6927 (1998).
Contamine, F., F. Faid, A. M. Wilhelm, J. Berlan, and H. Delmas, "Chemical Reactions Under Ultrasound: Discrimination of Chemical and Physical Effects," *Chem. Eng. Sci.*, **49**, 5865 (1994).
Couppis, E. C., and G. E. Klinzing, "Effect of Cavitation on Reacting Systems," *AIChE J.*, **20**, 485 (1974).
Dahlem, O., V. Demaiffe, V. Halloin, and J. Reisse, "Direct Sonication System Suitable for Medium Scale Sonochemical Reactors," *AIChE J.*, **44**, 2724 (1998).
Dahlem, O., J. Reisse, and V. Halloin, "The Radially Vibrating Horn: A Scaling up Possibility for Sonochemical Reactions," *Chem. Eng. Sci.*, **54**, 2829 (1999).
Dahnke, S., and F. Keil, "Modelling of Three-Dimensional Linear Pressure Fields in Sonochemical Reactors with Homogenous and Inhomogeneous Density Distribution of Cavitation Bubbles," *Ind. Eng. Chem. Res.*, **37**, 848 (1998a).
Dahnke, S., and F. Keil, "Modelling of Sound Fields in Liquids with a Non-homogenous Distribution of Cavitation Bubbles as a Basis for the Design of Sonochemical Reactors," *Chem. Eng. Tech.*, **21**, 873 (1998b).
Dahnke, S., and F. Keil, "Modelling of Linear Pressure Fields in Sonochemical Reactors Considering an Inhomogeneous Density Distribution of Cavitation Bubbles," *Chem. Eng. Sci.*, **54**, 2865 (1999).
Dahnke, S., K. M. Swamy, and F. J. Keil, "Modelling of Three Dimensional Pressure Fields in Sonochemical Reactors with an Inhomogeneous Density Distribution of Cavitation Bubbles. Comparison of Theoretical and Experimental Results," *Ultrason. Sonochem.*, **6**, 31 (1999a).
Dahnke, S., K. M. Swamy, and F. J. Keil, "A Comparative Study on the Modelling of Sound Pressure Field Distributions in a Sonoreactor with Experimental Investigation," *Ultrason. Sonochem.*, **6**, 221 (1999b).
Eller, A., and H. G. Flynn, "Generation of the Subharmonics of Order One Half by Bubbles in a Sound Field," *J. Acoust. Soc. Amer.*, **46**, 722 (1969).
Entezari, M. H., and P. Kruus, "Effect of Frequency on Sonochemical Reactions II. Temperature and Intensity Effects," *Ultrason. Sonochem.*, **3**, 19 (1996).
Esche, R., "Untersuchung der Schwingungskavitation in Flussigkeiten," *Acustica*, **2**, AB208 (1952).
Faid, F., M. Romdhane, C. Gourdon, A. M. Wilhelm, and H. Delmas, "A Comparative Study of Local Sensors of Power Ultrasound Effects: Electrochemical, Thermoelectrical and Chemical Probes," *Ultrason. Sonochem.*, **5**, 63 (1998).
Flynn, H. G., "Cavitation Dynamics I: Mathematical Formulation," *J. Acoust. Soc. Amer.*, **57**, 1379 (1975).
Gogate, P. R., "Cavitation: an Auxiliary Technique in Wastewater Treatment Schemes," *Adv. Environ. Res.*, in press (2001).
Gogate, P. R., and A. B. Pandit, "Engineering Design Methods for Cavitation Reactors I: Sonochemical Reactors," *AIChE J.*, **46**, 372 (2000).
Gogate, P. R., I. Z. Shirgaonkar, M. Sivakumar, P. Senthilkumar, N. P. Vichare, and A. B. Pandit, "Cavitation Reactors: Efficiency Analysis Using a Model Reaction," *AIChE J.*, , **47**, 2526 (2001a).
Gogate, P. R., S. Mujumdar, and A. B. Pandit, "Sonochemical Reactors for Waste Water Treatment Comparison Using Formic Acid Degradation as a Model Reaction," *Adv. Environ. Res.*, in press (2001b).
Gonze, E., Y. Gonthier, P. Boldo, and A. Bernis, "Standing Waves in a High Frequency Sonoreactor: Visualisation and Effects," *Chem. Eng. Sci.*, **53**, 523 (1998).
Gutierrez, M., and A. Henglein, "Chemical Action of Pulsed Ultrasound: Observation of Unprecedented Intensity Effect," *J. Phys. Chem.*, **94**, 3625 (1990).
Hua, I., and M. R. Hoffmann, "Optimisation of Ultrasonic Irradiation as an Advanced Oxidation Technology," *Environ. Sci. Technol.*, **31**, 2237 (1997).
Hung, H.-M., and M. R. Hoffmann, "Kinetics and Mechanism of the Sonolytic Degradation of Chlorinated Hydrocarbons: Frequency Effects," *J. of Phys. Chem. A*, **103**, 2734 (1999).
Keil, F., and S. Dahnke, "Numerical Calculation of Pressure Fields in Sonochemical Reactors," (in German), *Chem. Ing. Tech.*, **68**, 419 (1996).
Keil, F., and S. Dahnke, "Numerical Calculation of Pressure Fields in Sonochemical Reactors—Linear Effects in Homogenous Phase," *Period Polytech. Ser. Chem. Eng.*, **41**, 41 (1997a).
Keil, F., and S. Dahnke, "Numerical Calculation of Scale-Up Effects of Pressure Fields in Sonochemical Reactors—Homogenous Phase," *Hung. J. Ind. Chem.*, **25**, 71 (1997b).
Kotronarou, A., G. Mills, and M. R. Hoffmann, "Ultrasonic Irradiation of p-Nitrophenol in Aqueous Solutions," *J. Phys. Chem.*, **95**, 3630 (1991).
Kotronarou, A., G. Mills, and M. R. Hoffmann, "Decomposition of Parathion in Aqueous Solution by Ultrasonic Irradiation," *Environ. Sci. Technol.*, **26**, 1460 (1992).
Lindley, J., and T. J. Mason, "Use of Ultrasound in Chemical Synthesis," *Chem. Soc. Rev.*, **16**, 275 (1987).
Luche, J. L., *Synthetic Organic Sono-Chemistry*, Plenum Press, New York (1999).
Martin, C. J., and A. N. R. Law, "The Use of Thermistor Probes to Measure the Energy Distributions in the Bath," *Ultrasonics*, **18**, 127 (1980).
Mason, T. J., "Use of Ultrasound in Chemical Synthesis," *Ultrasonics*, **24**, 245 (1986).
Mason, T. J., and J. P. Lorimer, *Sonochemistry: Theory, Applications and Uses of Ultrasound in Chemistry*, Horwood, London (1988).
Mason, T. J., "Sonochemistry: Current Uses and Future Prospects in the Chemical and Processing Industries," *Philos. Trans. R. Soc. London A*, **357**, 355 (1999).
Matula, T. J., I. M. Hallaj, R. O. Cleveland, L. A. Crum, and R. A. Roy, "The Acoustic Emission from Single Bubble Sonoluminescence," *J. Acoust. Soc. Amer.*, **103**, 1377 (1998).
McCall, R. E., E. R. Lee, G. N. Mock, and P. L. Grady, "Improving Dye Yields of Vats on Cotton Fabric Using Ultrasound," *AATCC Book of Papers*, Philadelphia, p. 188 (1998).
Moholkar, V. S., A. B. Pandit, and M. M. C. G. Warmoeskerken, "Characterization and Optimization Aspects of a Sonic Reactor," ICEU-99, New Delhi, India (1999).
Moholkar, V. S., S. P. Sabale, and A. B. Pandit, "Mapping the Cavitation Intensity in an Ultrasonic Bath Using the Acoustic Emission," *AIChE J.*, **46**, 684 (2000).
Moholkar, V. S., and M. M. C. G. Warmoeskerken, "Modelling of the Acoustic Pressure Fields and the Distribution of the Cavitation Phenomena in a Dual Frequency Sonic Processor," *Ultrasonics*, **38**, 666 (2000).
Moss, W. C., D. A. Young, J. A. Harte, J. L. Levatin, B. F. Rozsnyai, G. B. Zimmerman, and I. H. Zimmerman, "Computed Optical Emissions from a Sonoluminescing Bubble," *Phys. Rev. E*, **59**, 2986 (1999).
Mujumdar, S., P. Senthil Kumar, and A. B. Pandit, "Emulsification by Ultrasound: Effect of Intensity on Emulsion Quality," *Indian J. Chem. Technol.*, **4**, 277 (1997).
Naidu, D. V., R. Rajan, R. Kumar, K. S. Gandhi, V. H. Arakeri, and S. Chandrasekaran, "Modelling of a Batch Sono-Chemical Reactor," *Chem. Eng. Sci.*, **49**(6), 377 (1994).
Neppiras, E., "Measurement of Acoustic Cavitation," *IEEE Trans. Sonics Ultrason.*, **SU-2**, 81 (1968).
Ondruschka, B., J. Lifka, and J. Hofmann, "Aquasonolysis of Ether: Effect of Frequency and Acoustic Power of Ultrasound," *Chem. Eng. Technol.*, **23**, 588 (2000).
Pandit, A. B., and J. B. Joshi, "Hydrolysis of Fatty Oils: Effect of Cavitation," *Chem. Eng. Sci.*, **48**, 3440 (1993).
Pandit, A. B., P. R. Gogate, and S. Mujumdar, "Ultrasonic Degradation of 2-4-6 Trichlorophenol in Presence of TiO_2 Catalyst," *Ultrason. Sonochem.*, **8**, 227 (2001).
Petrier, C., A. L. Gemal, and J. L. Luche, "Ultrasound in Organic Synthesis: 3. A Simple High Yield Modification of the Bouveault Reaction," *Tetrahedron Lett.*, **23**, 3361 (1982).
Petrier, C., J. L. Luche, and C. Dupuy, "Ultrasound in Organic Syn-

thesis 6: An Easy Preparation of Organozinc Reagents and Their Conjugate Addition to α-enones," *Tetrahedron Lett.*, **25**, 3463 (1984).
Petrier, C., and J. L. Luche, "Ultrasonically Improved Reductive Properties of an Aqueous Zn-$NiCl_2$ System: 1. Selective Reduction of α-β Unsaturated Carbonyl Compounds," *Tetrahedron Lett.*, **28**, 2347 (1987).
Petrier, C., M. Micolle, G. Merlin, J.-L. Luche, and G. Reverdy, "Characteristics of Pentachlorophenate Degradation in Aqueous Solutions by Means of Ultrasound," *Environ. Sci. Technol.*, **26**, 1639 (1992).
Plesset, M. S., "Dynamics of Cavitating Bubble," *J. Appl. Mech. Trans. ASME*, **16**, 277 (1949).
Pugin, B., "Qualitative Characterization of Ultrasound Reactors for Heterogeneous Sonochemistry," *Ultrasonics*, **25**, 49 (1987).
Rajan, R., R. Kumar, and K. S. Gandhi, "Modelling of Sonochemical Decomposition of CCl_4 in Aqueous Solutions," *Environ. Sci. Technol.*, **32**, 1128 (1998a).
Rajan, R., R. Kumar, and K. S. Gandhi, "Modelling of Sonochemical Oxidation of the Water-KI-CCl_4 System," *Chem. Eng. Sci.*, **53**, 255 (1998b).
Rathi, N. H., G. N. Mock, R. E. McCall, and P. L. Grady, "Ultrasound Aided Open Width Washing of Mercerised 100% Cotton Twill Fabric," *AATCC Book of Papers*, Atlanta, GA, 254 (1997).
Ratoarinoro, C., A. M. Wilhelm, and H. Delmas, "Power Measurements in Sonochemistry," *Ultrasonics Sonochem.*, **2**, S43 (1995).
Romdhane, M., C. Gourdon, and G. Casamatta, "Local Investigation of Some Ultrasonic Devices by Means of a Thermal Sensor," *Ultrasonics*, **33**, 221 (1995a).
Romdhane, M., C. Gourdon, and G. Casamatta, "Development of a Thermoelectric Sensor for Ultrasonic Intensity Measurement," *Ultrasonics*, **33**, 139 (1995b).
Romdhane, M., A. Gadri, F. Contamine, C. Gourdon, and G. Casamatta, "Experimental Study of the Ultrasound Attenuation in Chemical Reactors," *Ultrason. Sonochem.*, **4**, 235 (1997).
Rong, L., Y. Kojima, S. Koda, and H. Nomura, "Simple Quantification of Ultrasonic Intensity Using Aqueous Solution of Phenolphthalein," *Ultrasonics Sonochem.*, **8**, 11 (2001).
Saksena, T. K., "Variation of Reliable Measurement of Ultrasonic Power and Cavitation in Liquid," *J. Acoustic Soc. India*, **8**, 12 (1983).
Save, S. S., A. B. Pandit, and J. B. Joshi, "Microbial Cell Disruption: Role of Cavitation," *Chem. Eng. J.*, **55**, B67 (1994).
Senthilkumar, P., M. Sivakumar, and A. B. Pandit, "Experimental Quantification of Chemical Effects of Hydrodynamic Cavitation," *Chem. Eng. Sci.*, **55**, 1633 (2000).
Serpone, N., R. Terzian, H. Hidaka, and E. Pelizzetti, "Ultrasonic Induced Dehalogenation and Oxidation of 2-, 3- and 4-Chlorophenol in Air-Equilibrated Aqueous Media: Similarities with Irradiated Semiconductor Particulates," *J. Phys. Chem.*, **98**, 2634 (1994).
Seymore, J. D., and R. B. Gupta, "Oxidation of Aqueous Pollutants Using Ultrasound-Salt Induced Enhancement," *Ind. Eng. Chem. Res.*, **36**, 3453 (1997).
Shah, Y. T., A. B. Pandit, and V. S. Moholkar, *Cavitation Reaction Engineering*, Kwarner Publishers, New York (1999).
Shima, A., and Y. Tomita, "The Behaviour of a Spherical Bubble in Mercury," *Report 2. Rep. Inst. High Speed Mech.*, Vol. 39, Tohoku Univ., Tohoku, Japan, p. 19 (1979).
Shirgaonkar, I. Z., and A. B. Pandit, "Degradation of Aqueous Solution of Potassium Iodide and Sodium Cyanide in Presence of Carbon Tetrachloride," *Ultrasonics Sonochem.*, **4**, 245 (1997).
Shirgaonkar, I. Z., R. R. Lothe, and A. B. Pandit, "Comments on the Mechanism of Microbial Cell Disruption in High Pressure and High Speed Devices," *Biotechnol. Prog.*, **14**, 857 (1998).
Sivakumar, M., and A. B. Pandit, "Ultrasound Enhanced PTC Conversion of Benzamide to Benzonitrile," *Synthetic Commun.*, **31**, 2583 (2001a).
Sivakumar, M., and A. B. Pandit, "Ultrasound Enhanced Degradation of Rhodamine B: Optimisation with Power Density," *Ultrasonics Sonochem.*, **8**, 233 (2001b).
Sivakumar, M., P. Senthilkumar, S. Mujumdar, and A. B. Pandit, "Ultrasound Mediated Alkaline Hydrolysis of Methyl Benzoate: Reinvestigation with Crucial Parameters," *Ultrason. Sonochem.*, **9**, 25 (2002a).
Sivakumar, M., P. A. Tatake, and A. B. Pandit, "Kinetics of p-Nitrophenol Degradation: Effect of Reaction Conditions and Cavitational Parameters for a Multiple Frequency System," *Chem. Eng. J.*, **85**, 327 (2002b).
Sochard, S., A. M. Wilhelm, and H. Delmas, "Gas-Vapour Bubble Dynamics and Homogenous Sonochemistry," *Chem. Eng. Sci.*, **53**, 239 (1998).
Soudagar, S. R., and S. D. Samant, "Semiquantitative Characterization of Ultrasonic Cleaner Using a Novel Piezoelectric Pressure Intensity Measurement Probe," *Ultrason. Sonochem.*, **2**, S49 (1995).
Srinivasan, R., I. Z. Shirgaonkar, and A. B. Pandit, "Effect of Sonication on Crystal Properties," *Sep. Sci. Technol.*, **30**, 2239 (1995).
Storey, B. D., and A. J. Szeri, "Mixture Segregation Within Sonoluminescence Bubbles," *J. Fluid Mech.*, **396**, 203 (1999).
Storey, B. D., and A. J. Szeri, "Water Vapour, Sonoluminescence and Sonochemistry," *Proc. Roy. Soc. London A*, **456**, 1685 (2000).
Suslick, K. S., *Ultrasound: Its Chemical, Physical and Biological Effects*, VCH, New York (1988).
Suslick, K. S., M. M. Mdleleni, and J. T. Reis, "Chemistry Induced by Hydrodynamic Cavitation," *J. Amer. Chem. Soc.*, **119**, 9303 (1997).
Takami, A., S. Kato, A. Shimono, and K. Seichiro, "Uptake Coefficient of OH· Radical on Aqueous Surface," *Chem. Phys.*, **231**, 215 (1998).
Tatake, P. A., and A. B. Pandit, "Modelling and Experimental Investigation into Cavity Dynamics and Cavitational Yield: Influence of Multiple Frequency Ultrasound Sources," *Chem. Eng. Sci.*, (2001).
Thakore, K. A., "Physico-Chemical Study on Applying Ultrasonics in Textile Dyeing," *Amer. Dyestuff Rep.*, **79**, 45 (1990).
Thoma, G., J. Swofford, V. Popov, and M. Som, "Sonochemical Destruction of Dichloromethane and o-Dichlorobenzene in Aqueous Solution Using a Nearfield Acoustic Processor," *Adv. Environ. Res.*, **1**, 178 (1997).
Thompson, L. H., and L. K. Doraiswamy, "Sonochemistry: Science and Engineering," *Ind. Eng. Chem. Res.*, **38**, 1215 (1999).
Tomita, Y., and A. Shima, "Mechanisms of Impulsive Pressure Generation and Damage Pit Formation by Bubble Collapse," *J. Fluid Mech.*, **169**, 535 (1986).
Trabelsi, F., H. Ait-lyazidi, J. Berlan, P. L. Fabre, H. Delmas, and A. M. Wilhelm, "Electrochemical Determination of the Active Zones in a High Frequency Ultrasonic Reactor," *Ultrasonics Sonochem.*, **3**, S125 (1996).
Tsochatzidis, N. A., P. Guiraud, A. M. Wilhelm, and H. Delmas, "Determination of Velocity, Size and Concentration of Ultrasonic Cavitation Bubbles by the Phase-Doppler Technique," *Chem. Eng. Sci.*, **56**(5), 1831 (2001).
Vichare, N. P., P. R. Gogate, and A. B. Pandit, "Optimization of Hydrodynamic Cavitation Using a Model Reaction," *Chem. Eng. Technol.*, **22**, 683 (2000).
Weavers, L. K., F. H. Ling, and M. R. Hoffmann, "Aromatic Compound Degradation in Water Using a Combination of Sonolysis and Ozonolysis," *Environ. Sci. Technol.*, **32**, 2727 (1998).
Weissler, A., "Chemical Effect of Ultrasonic Waves: Oxidation of Potassium Iodide Solution by Carbon Tetrachloride," *J. Acoust. Soc. Amer.*, **72**, 1769 (1950).
Yechmenev, V. G., E. J. Blanchard, and A. H. Lambert, "Study of the Influence of Ultrasound on Enzymatic Treatment of Cotton Fabric," *AATCC Book of Papers*, Philadelphia, p. 472 (1998).
Yechmenev, V. G., E. J. Blanchard, and A. H. Lambert, "Study of the Influence of Ultrasound on Enzymatic Treatment of Cotton Fabric," *Text. Color. Chem. Amer. Dyestuff Rep.*, **1**, 47 (1999).
Young, F. R., *Cavitation*, McGraw Hill, London (1989).

Manuscript received May 10, 2001, and revision received Dec. 4, 2001.